Oklahoma Department of Transportation
200 NE 21st Street, Oklahoma City, OK 73105-3204

FINAL REPORT ~ FHWA-OK-14-06

REAL TIME MONITORING OF SLOPE STABILITY IN EASTERN OKLAHOMA

Amy B. Cerato, Ph.D., P.E.
Yang Hong, Ph.D.
Xiado Yu
Xiaogang He
Wassim Tabet
School of Civil Engineering and Environmental Science
College of Engineering
The University of Oklahoma

January 2014

Oklahoma Department of Transportation

REAL TIME MONITORING OF SLOPE STABILITY IN EASTERN OKLAHOMA

FINAL REPORT ~ FHWA-OK-14-08
ODOT SP&R ITEM NUMBER 2241

Submitted to:
John R. Bowman, P.E.
Planning & Research Division Engineer
Oklahoma Department of Transportation

Submitted by:
Amy Cerato, Ph.D., P.E.
Yang Hong, Ph.D.
Xiaodi Yu, Research Assistant
Xiaogang He, Research Assistant
Wassim Tabet, Research Assistant

School of Civil Engineering and Environmental Science (CEES)
The University of Oklahoma

January 2014

TECHNICAL REPORT DOCUMENTATION PAGE

1. REPORT NO. FHWA-OK-14-06	2.GOVERNMENT ACCESSION NO.	3. RECIPIENT'S CATALOG NO.
4. TITLE AND SUBTITLE Real-Time Monitoring of Slope Stability in Southeastern Oklahoma		5. REPORT DATE 1/31/2014
		6. PERFORMING ORGANIZATION CODE
7. AUTHOR(S) Amy B. Cerato, Yang Hong, Xiaodi Yu, Xiaogang He, Wassim Tabet		8.PERFORMING ORGANIZATION REPORT
9. PERFORMING ORGANIZATION NAME AND ADDRESS The University of Oklahoma School of Civil Engineering & Environmental Science 202 W. Boyd Street, Room 334 Norman, OK 73019		10. WORK UNIT NO.
		11. CONTRACT OR GRANT NO. ODOT SP&R Item Number 2241
12. SPONSORING AGENCY NAME AND ADDRESS Oklahoma Department of Transportation Planning and Research Division 200 N.E. 21st Street, Room 3A7 Oklahoma City, OK 73105		13. TYPE OF REPORT AND PERIOD COVERED Final Report 10/1/2011 - 12/31/13
		14. SPONSORING AGENCY CODE
15. SUPPLEMENTARY NOTES		

16. ABSTRACT

There were three primary objectives of the proposed research. The first was to establish a comprehensive landslide database, the second was to create a first- cut regional landslide map and the third was to relate safe and stable constructed slope geometry to soil type and geologic setting with site-based in-situ monitoring and modeling experiments.

Accomplishing the project objectives involved collecting historical and current landslide information from around the state, as well as climate, rainfall history, geology and topography information for recorded landslide sites. From this comprehensive database, a landslide susceptibility map was derived. In addition, in situ measuring equipment was used to monitor a selected slide to verify a site-based landslide modeling system.

17. KEY WORDS Slope stability, landslides, GIS, hazard mapping	18. DISTRIBUTION STATEMENT No restrictions. This publication is available from the Planning & Research Div., Oklahoma DOT.		
19. SECURITY CLASSIF. (OF THIS REPORT) Unclassified	20. SECURITY CLASSIF. (OF THIS PAGE) Unclassified	21. NO. OF PAGES 91	22. PRICE N/A

SI* (MODERN METRIC) CONVERSION FACTORS

APPROXIMATE CONVERSIONS TO SI UNITS				
SYMBOL	**WHEN YOU KNOW**	**MULTIPLY BY**	**TO FIND**	**SYMBOL**
LENGTH				
in	inches	25.4	millimeters	mm
ft	feet	0.305	meters	m
yd	yards	0.914	meters	m
mi	miles	1.61	kilometers	km
AREA				
in^2	square inches	645.2	square millimeters	mm^2
ft^2	square feet	0.093	square meters	m^2
yd^2	square yard	0.836	square meters	m^2
ac	acres	0.405	hectares	ha
mi^2	square miles	2.59	square kilometers	km^2
VOLUME				
fl oz	fluid ounces	29.57	milliliters	mL
gal	gallons	3.785	liters	L
ft^3	cubic feet	0.028	cubic meters	m^3
yd^3	cubic yards	0.765	cubic meters	m^3
NOTE: volumes greater than 1000 L shall be shown in m^3				
MASS				
oz	ounces	28.35	grams	g
lb	pounds	0.454	kilograms	kg
T	short tons (2000 lb)	0.907	megagrams (or "metric ton")	Mg (or "t")
TEMPERATURE (exact degrees)				
^oF	Fahrenheit	5 (F-32)/9 or (F-32)/1.8	Celsius	^oC
ILLUMINATION				
fc	foot-candles	10.76	lux	lx
fl	foot-Lamberts	3.426	candela/m^2	cd/m^2
FORCE and PRESSURE or STRESS				
lbf	poundforce	4.45	newtons	N
lbf/in^2	poundforce per square inch	6.89	kilopascals	kPa

APPROXIMATE CONVERSIONS FROM SI UNITS				
SYMBOL	**WHEN YOU KNOW**	**MULTIPLY BY**	**TO FIND**	**SYMBOL**
LENGTH				
mm	millimeters	0.039	inches	in
m	meters	3.28	feet	ft
m	meters	1.09	yards	yd
km	kilometers	0.621	miles	mi
AREA				
mm^2	square millimeters	0.0016	square inches	in^2
m^2	square meters	10.764	square feet	ft^2
m^2	square meters	1.195	square yards	yd^2
ha	hectares	2.47	acres	ac
km^2	square kilometers	0.386	square miles	mi^2
VOLUME				
mL	milliliters	0.034	fluid ounces	fl oz
L	liters	0.264	gallons	gal
m^3	cubic meters	35.314	cubic feet	ft^3
m^3	cubic meters	1.307	cubic yards	yd^3
MASS				
g	grams	0.035	ounces	oz
kg	kilograms	2.202	pounds	lb
Mg (or "t")	megagrams (or "metric ton")	1.103	short tons (2000 lb)	T
TEMPERATURE (exact degrees)				
^oC	Celsius	1.8C+32	Fahrenheit	^oF
ILLUMINATION				
lx	lux	0.0929	foot-candles	fc
cd/m^2	$candela/m^2$	0.2919	foot-Lamberts	fl
FORCE and PRESSURE or STRESS				
N	newtons	0.225	poundforce	lbf
kPa	kilopascals	0.145	poundforce per square inch	lbf/in^2

*SI is the symbol for the International System of Units. Appropriate rounding should be made to comply with Section 4 of ASTM E380.

Acknowledgments

The success of this research project, which had a significant field surveying, sampling and data collection component, was largely due to the cooperation and support of ODOT Division and Resident personnel. The principal investigators from OU gratefully acknowledge and thank the following persons:

ODOT Materials Division

Christopher Clarke, P.E.

ODOT Division 1

Troy Travis and Mickey Bennett, Field Maintenance Manager

ODOT Division 2

Brian Taylor

ODOT Division 3

Bill Wilkinson, Division Maintenance Engineer and Wendy Ross

Natural Resources Conservation Service (NRCS)/US Department of Agriculture (USDA) National GeoSpatial Management Center

Collin McCormick, Supervisory Cartographer

Steve Nechero, Cartographer

Table of Contents

List of Tables

List of Figures

Chapter 1: Introduction

This final report describes a summary of work accomplished during the two year project period. There were three primary objectives of the proposed research. The first was to establish a comprehensive landslide database, the second was to create a first- cut regional landslide map and the third was to relate safe and stable constructed slope geometry to soil type and geologic setting with site-based in-situ monitoring and modeling experiments.

Accomplishing the project objectives involved collecting historical and current landslide information from around the state, as well as climate, rainfall history, geology and topography information for recorded landslide sites. From this comprehensive database, a landslide susceptibility map was derived. In addition, in situ measuring equipment was used to monitor a selected slide to verify a site-based landslide modeling system.

Background

The goals of this research project were to assist the state in understanding, recognizing, and addressing landslide prone areas by creating a functional landslide hazard map that may be used by ODOT and others when building and maintaining infrastructure to predict and prevent future transportation corridor blockages (slides). The intent of this research was to establish a landslide database that will lay the groundwork for a future real-time monitoring and prediction system for Oklahoma Transportation officials to use as a warning system to minimize life-lost as well as interruptions to critical transportation corridors. While it is recognized that slope failures are based on specific, localized properties that are (should be) measured and designed for, having the predictive power to identify what existing slopes are more likely to fail, and what areas (geological, topographical, climatological) are prone to failure at commonly used slopes, gives transportation officials the tools to identify slopes, warn stakeholders, and even prevent landslides from occurring.

Objectives

The objectives and specific tasks of the proposed research which support the long term goal were

A. To establish a comprehensive landslide database.
B. Based on the comprehensive database, create a first-cut regional landslide map.
C. To relate safe and stable constructed slope geometry to soil type and geologic setting with site-based in-situ monitoring and modeling experiments.

Chapter 2: Results of Research Program

Objective A

Task A1: Historical and Current Landslide Identification

Division 1, Division 2 and 3 provided a total of 23 landslide/problematic locations to study, all of which the project team visited and documented. One location in Division 2 along Route 70, West of Idabel, was chosen for instrumentation, and all soil information and testing is shown in Appendix A. The remaining locations are shown in Appendix B along with specific notes on size, location, soil type and damage extent. Many of these slide areas had been fixed already, or in the process of being fixed (e.g., Route 82) and showing no continuous movement. In those cases, the project team simply noted the location and took pictures of the repair. In other cases, the landslides were a continuous maintenance issue (e.g., pavement overlays, restriping, etc.). In those cases, the project team measured the extent of the slide when possible and attempted to take soil samples, along with recording pictures of the head scarp and extent of the slide. The current landslides are noted in Table 1.

Table 1. Current and Recurring Landslides Identified by Division 1, 2 and 3 Engineers:

Division 1	Division 2	Division 3
Route 9, 1 mile east of Turnpike; several miles west of Eufala, on south side of road	Route 271, 2 miles north of Junction 144	Route 9, 3.5 miles East of Wetumka
Route 2, 4 miles south of junction with Route 31; also north of Robber's Cave St. Park	Route 271, near Talimena State Park	I-40E, 1 mile before Exit 200 (Seminole) on south side backslope
west side of Route 10, about 5 miles south of the intersection with Route 62 (south of Fort Gibson)	Route 82, north of Red Oak on West side of highway (one is fixed, the other is not)	
Route 80 just south of Fort Gibson Dam, on west side of Route 80N	Route 70, west of Idabel in McCurtain County, on north side of Road (This site was chosen for instrumentation)	
Route 75, 0.6 miles north of Preston Road at the first guard rail on right (east).		

This serves as a historical and current record of problematic areas within those divisions so that future efforts can be directed at the most troublesome locations. The

USGS provided us with old maps noting approximately 80 historical landslide locations. Unfortunately, from the scale of the map, and the age of the landslides, the project team was unable to positively identify landslides using satellite images and field visits on some of the locations. We used these locations, however, in generating the landslide hazard map. All of the locations noted are shown on the GIS maps later in this report.

Task A2: Information Gathering on Identified Landslide Locations

The Natural Resources Conservation Service (NRCS) Geospatial Data Management Center in Fort Worth, TX provided all of our LiDAR data. The 5m DEM data and 30 cm imagery data covering the landslide locations were purchased from East View Geospatial, Inc. The Oklahoma Mesonet stations were utilized for historical rainfall data.

Task A3: Establish an Oklahoma Landslide Inventory Database

The field trip data, the USGS historical landslide data, along with all the climate, topography, soil type, rainfall, etc., data, were sorted into a database.

Objective B

Task B1: Derive Landslide Controlling Factors from Database

Landslide occurrence is determined by complex interactions among large number of factors, such as geologic feature, geomorphology, land cover, soil properties and hydrology. All these factors can be classified into two categories: static factors and dynamic factors. Static factors include the geologic features, geomorphology, land cover and soil characters which are kept stable for a relatively long period of time. When we talk about dynamic factors, it refers to the trigger factors of landslides, mainly rainfall and earthquakes (Dai et al 2002). When mapping landslides susceptibility, only static factors are considered. In this study, four major layers were selected to generate the Oklahoma landslide susceptibility map, including *slope, elevation, land cover type* and *soil texture* data.

The National Elevation Dataset (NED) (http://ned.usgs.gov/) was used in this study, which is the primary elevation data product of USGS. The NED is updated on a nominal two months cycle to integrate newly available improved elevation source data. It is the best continuous dataset all over the United States. NED data are available at resolution of 1 arc-second (about 30 meters) and 1/3 arc-second (about 10 meters) and in limited areas at 1/9 arc-second (about 3 meters). The absolute vertical accuracy of NED data, which is expressed as the root mean square error (RMSE), is 2.44 meters. Figure 1 shows the 10-meter mosaic DEM of Oklahoma State from NED.

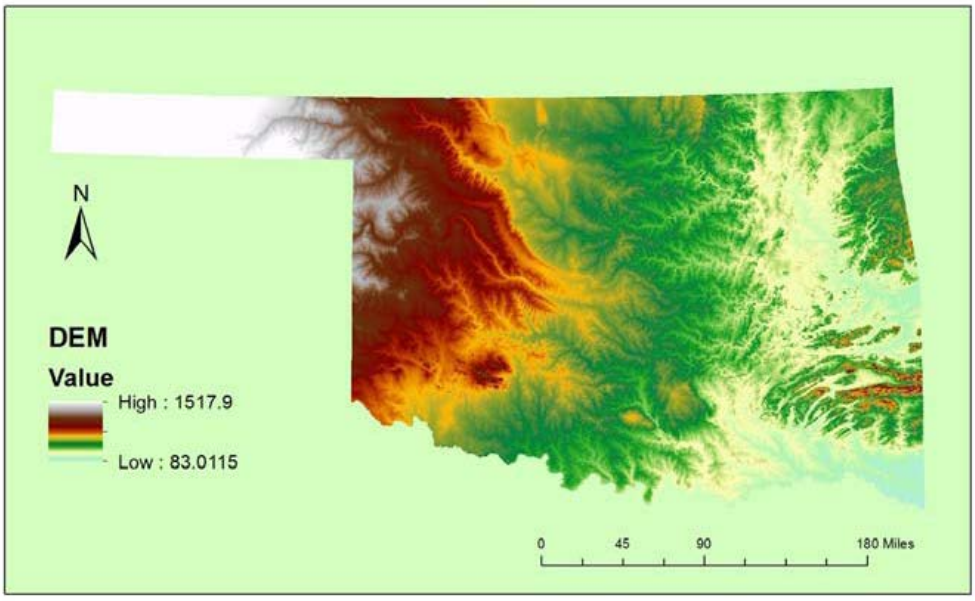

Figure 1: 30m NED Digital Elevation Model in Oklahoma.

The most direct information provided by DEM is elevation. Other than elevation, many topographic factors can be derived by DEM, including slope, slope aspect, hill shading, slope curvature and so on. Furthermore, slope, the most important factor in landslides susceptibility analysis, is prepared from DEM. Figure 2 shows the slope distribution through the whole state.

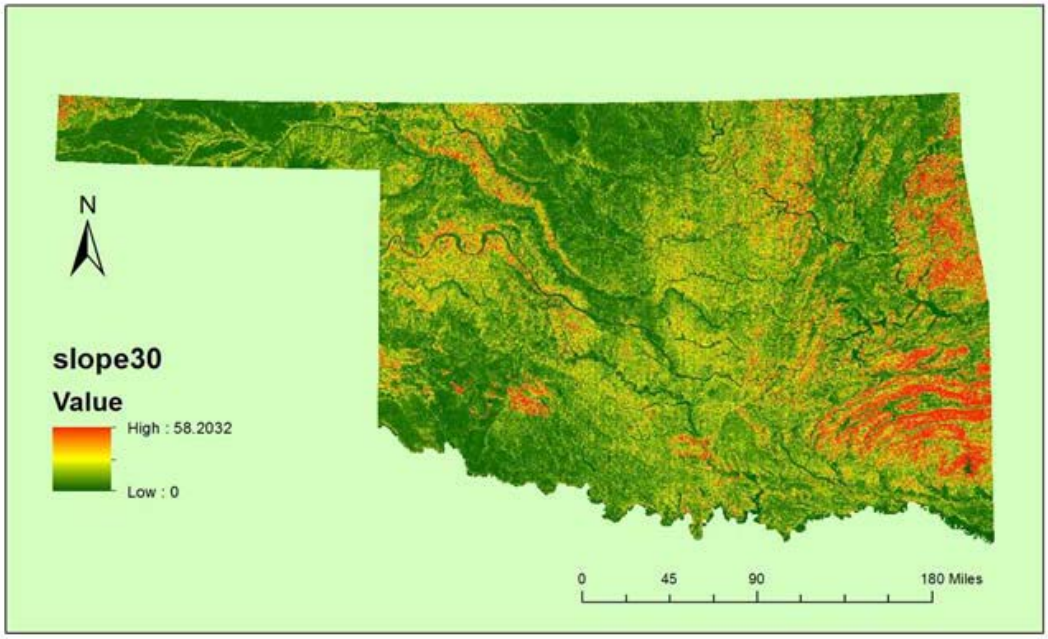

Figure 2: Slope derived from DEM.

The land cover data used in this study is National Land Cover Database 2006 (NLCD 2006) from USGS. This dataset is generated form Landsat Enhance Thematic

Mapper+ (ETM+) by using unsupervised classification method. NLCD land cover data has a spatial resolution of 30-meter. 15 different types of Land Cover exist in Oklahoma, which are shown in Figure 3.

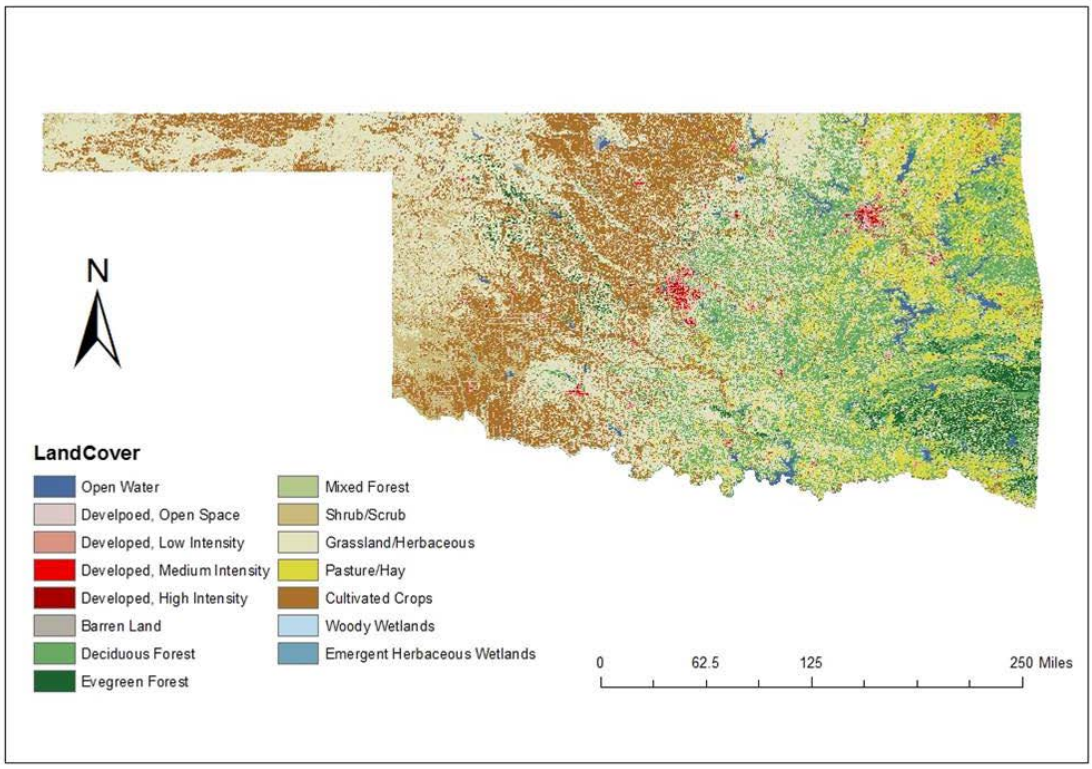

Figure 3. 30m National Land Cover Dataset from USGS.

State Soil Geographic Data Base (STATSGO) is produced by the United States Department of Agriculture - Natural Resource Conservation Service (USDA-NRCS). It consists of georeferenced digital map data and associated digital tables of attribute data. The STATSGO data are vector data. They cannot be directly used in gridded based studies, where soil data are most commonly used. The Soil Information for Environmental Modeling and Ecosystem Management is a mission done by Pennsylvania State University to provide soil information in understandable forms. Based on STATSGO, they have developed the gridded 1-km Multi-Layer Soil Characteristics Dataset that can be easily used in modeling study. The main soil data downloaded from this website is soil texture type for the Oklahoma State, which is shown in Figure 4.

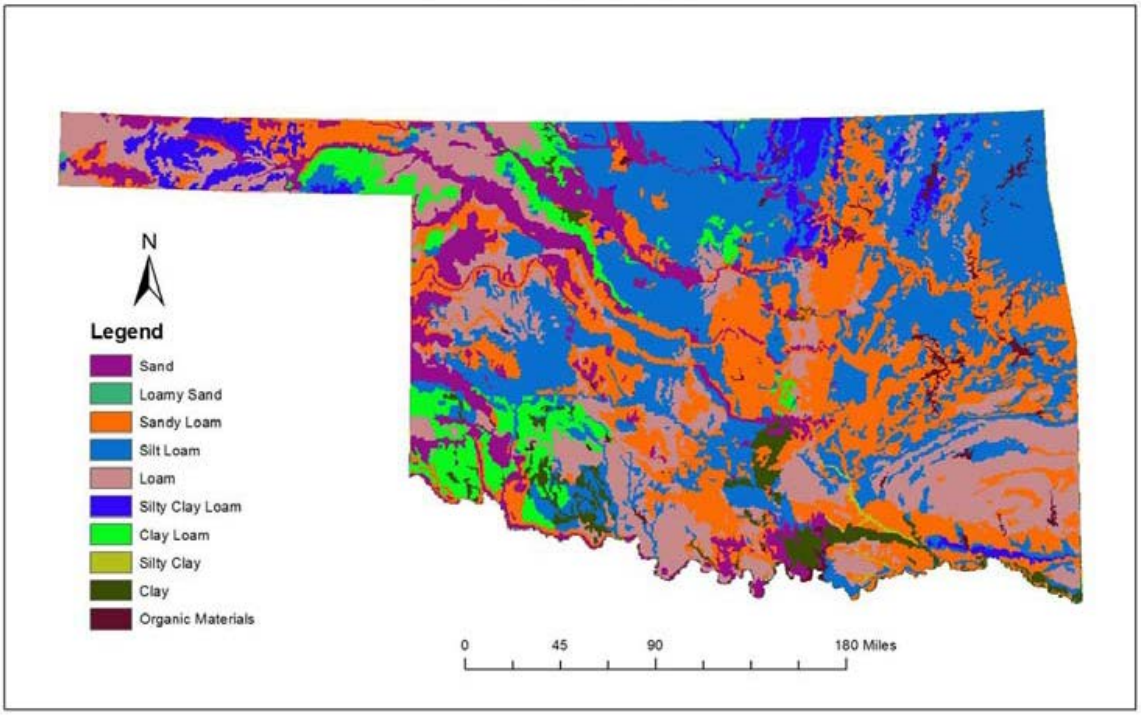

Figure 4. STATSGO soil texture data.

All these selected layers will be normalized into susceptibility values that range from 0 to 1, with 0 standing for no risk of landslide and 1 standing for high risk. For the layers having continuous values, fuzzy membership will be applied to each layer. For layers that have discrete values, reclassification will be done according to their physical characteristics, literature review and preview experience.

On the relationship between landslides and slope, Bathrellos et al. (2009) found that steep slopes (> 30 degree) had the maximum frequency of landslides, followed by moderately steep slope (20 to 30 degree). Gemitzi et al. (2011) also pointed out that maximum frequency was reached in 35-40 degree category, followed by a decrease in the >40 degree category. Based on the previous study, 30 to 40 degree is selected as the most susceptible slope to landslides. Slope will be reclassified using the following condition statement: Con("Slope" < 30, "Slope"/30.0, Con("Slope"<40, 1, (90 - "Slope")/(90.0 - 40.0))).

When considering the relationship between elevation and landslides, several studies show that the higher the elevation (Hong et al. 2007), the higher it is susceptible to landslides. However, in Oklahoma, elevation alone does not predict landslides, as the entire western part of the state is at an elevation near 4000-5000 feet, yet, not a lot of landslides occur because the topography is not conducive, and so elevation is given much less weight in this study.

In Hong et al. (2006), numerical values are assigned to different land cover types using MODIS land cover classification map. Even though these two land cover classification schemes are different between MODIS and ETM+ images, we can reclassify the NLCD map based on the similarities of these two maps (Table 2).

Table 2. Numerical values assigned to different land cover types.

Category	Land Cover Type	Value
1	Open water	0
2	Developed, Open Spaces	1.0
3	Developed, Low Intensity	1.0
4	Developed, Medium Intensity	0.7
5	Developed, High Intensity	0.7
6	Barren Land	0.9
7	Deciduous Forest	0.2
8	Evergreen Forest	0.1
9	Mixed Forest	0.3
10	Shrub/Scrub	0.4
11	Grassland/Herbaceous	0.5
12	Pasture/Hay	0.6
13	Cultivated Crops	0.7
14	Woody Wetlands	0.1
15	Emergent Herbaceous Wetlands	0.1

Godt et al. (2008) found that a combination of low soil cohesion and a low angle of internal friction will greatly increase the probability of landslide occurrence. Thus silty clay loam is the most vulnerable to landslides. However, in Oklahoma, most of the landslides surveyed occurred in clay deposits, with swelling capacity, and so clay soil was also given a higher weight. Also, drainage capacity should be considered when assigning values to each soil texture type. Poor drainage increases the downward weight of soil by holding more water than it releases. For example, sands have low landslide susceptibility because of a high drainage capacity. Table 3 shows different weight values to different soil texture types.

Table 3. Numerical values assigned to different soil texture types.

Category	Soil Texture Type	Value
1	Sand	0.2
2	Loamy Sand	0.4
3	Sandy Loam	0.8
4	Silt Loam	0.6
5	Loam	0.6
6	Silt Clay Loam	0.8
7	Clay Loam	0.8
8	Silt Clay	0.2
9	Clay	1.0
10	Water	0

Task B2: Classify Landslide-Controlling Factors

Landslide susceptibility hazard maps can be derived using the multi-thematic geospatial datasets. Then each thematic map will be assigned a weight according to its effect on slope stability. Weighted Linear Combination (WLC) is a method where landslide controlling factors can be combined by applying primary- and second-level weights (Ayalew et al., 2004). In this study, landslide susceptibility values will be

derived by WLC. Four key factors are selected which include *slope, soil texture type, land cover and elevation*. According to a previous study, slope and soil texture type are primary-level parameters, while land cover type and elevation are second-level parameters. One of the best combinations is (0.5, 0.25, 0.15, 0.1) for the four parameters, respectively.

According to the field survey, most landslides occurred in clayey soil. Layer 7 in this dataset is the most representative, and therefore it was used in this research. However, at depth of 60 cm, some of the soil pixels are classified as bedrock or others, which make assigning rating values complicated. To solve this problem, layer 2 is used to fill these cells. Thus, the final soil texture data used in this study is a combination of layer 7 and layer 2 (Figure 5). Soil with fine texture (clayey soil) has small pores and drains water gradually. This means that clayey soil holds water more than sandy soil. Hence, clayey soil is more susceptible to landslides because this soil can retain more water causing an increase in the soil mass weight.

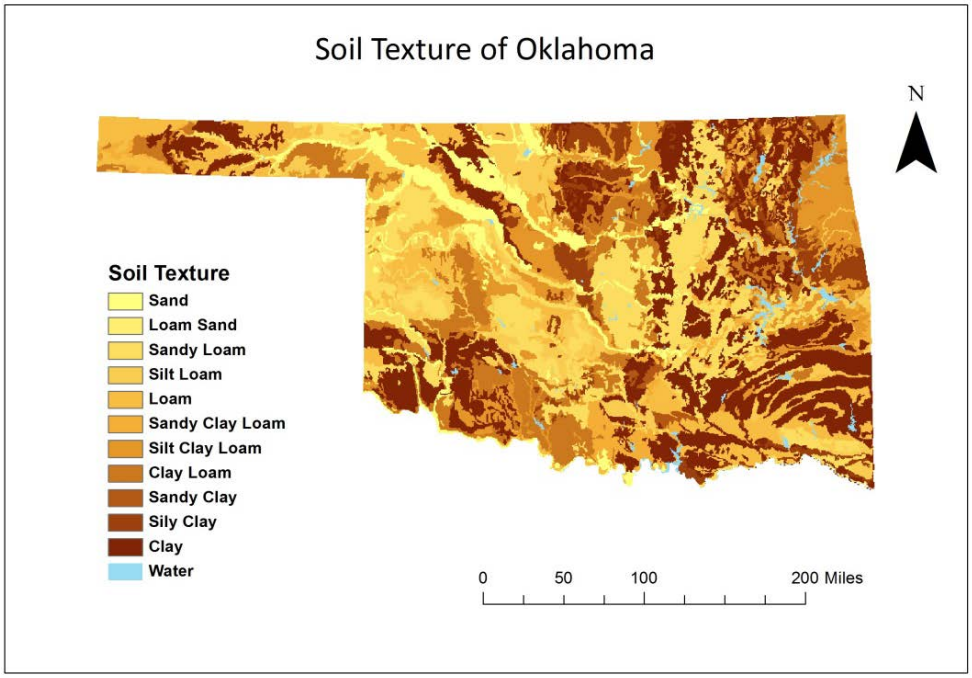

Figure 5. Multi-layer combined soil layer data.

According to the percentage of clay in each soil texture types, the ratings are assigned as shown in Table 4.

Table 4. Soil texture type rating according to clay percentage.

Soil Types	Rating
Water	0
Sand, Loamy sand, Silt	0.2
Sandy loam, Silt loam, Loam	0.4
Sandy clay loam, Silty clay loam, clay loam	0.6
Sandy clay, Silty clay	0.8
Clay	1

Task B3: Derive Landslide Susceptibility Map

Figure 6 shows the landslide susceptibility map of Oklahoma using the combined soil texture layer and new rating values. The highest risk area is at southeastern corner of this state. Histograms are created based on the map statistics and the ODOT landslide sites statistics (Figure 7). For 23 landslide events provided by ODOT, 19 are in category high or very high, which demonstrates strong ability of GIS-based weighted linear combination model in predicting landslide hotspots. The other 4 sites which are in low and medium categories are investigated using the input datasets. Results show that slope is the main reason that contributes to this result. For all the four sites, the slope values range from 3 degrees to 8.5 degrees, resulting in the very low rating in slope layer.

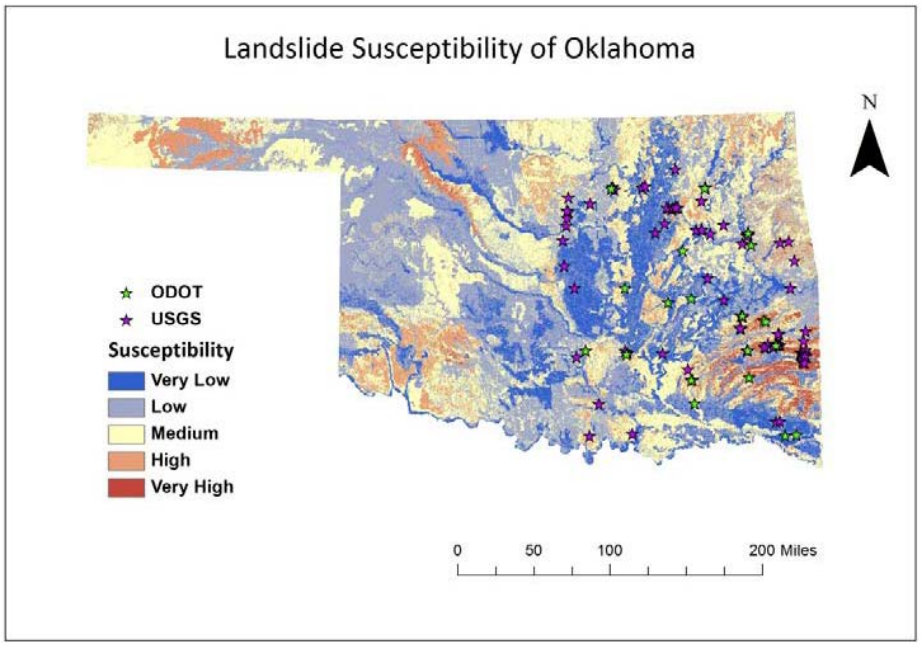

Figure 6. Updated landslide susceptibility map.

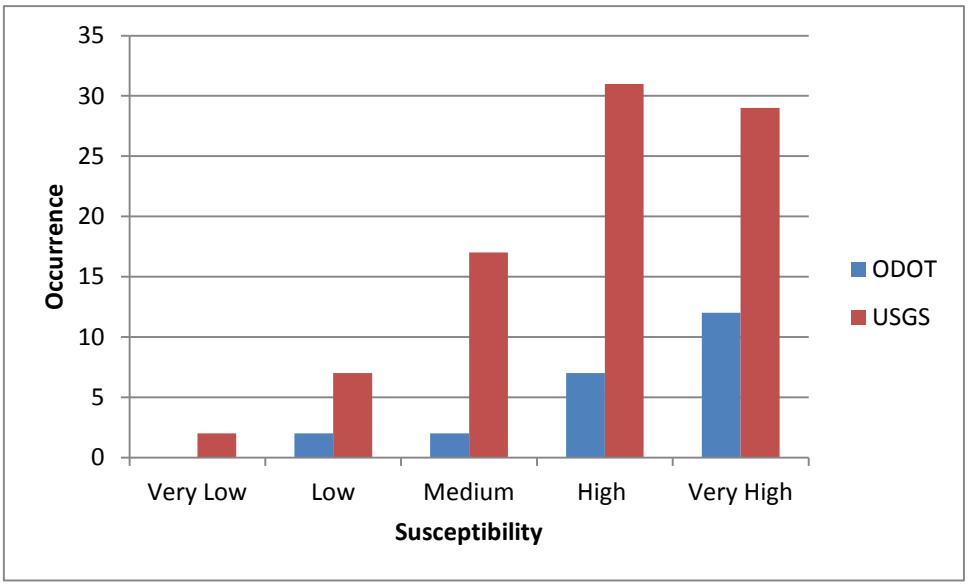

Figure 7. Result statistics of the state map and landslide sites.

Objective C

Task C1: Install in situ Measuring Equipment into chosen Landslide Location

The landslide on Route 70, near Idabel, OK, was chosen as one of the instrumentation sites. The weather station was installed in October 2012 and two inclinometers were installed five feet apart in the same cross-section in September 2013 (Figures 8, 9 and 10). The Materials Division took the initial inclinometer reading and has been taking readings once per month since installation. The instruments of the weather station include sensors to quantify rainfall, air temperature, relative humidity, wind speed, wind direction, solar radiation, and volumetric water content at three depths in the soil profile. At various times prior to, during and after installing the weather station, hand auger borings were advanced up to 10 feet in depth and samples were collected for moisture content determination and soil property tests. Laboratory testing included basic physical and index property tests including grain-size distribution, liquid and plastic limits. Strength tests, including triaxial and direct shear, were performed as well. All data are located in Appendix A.

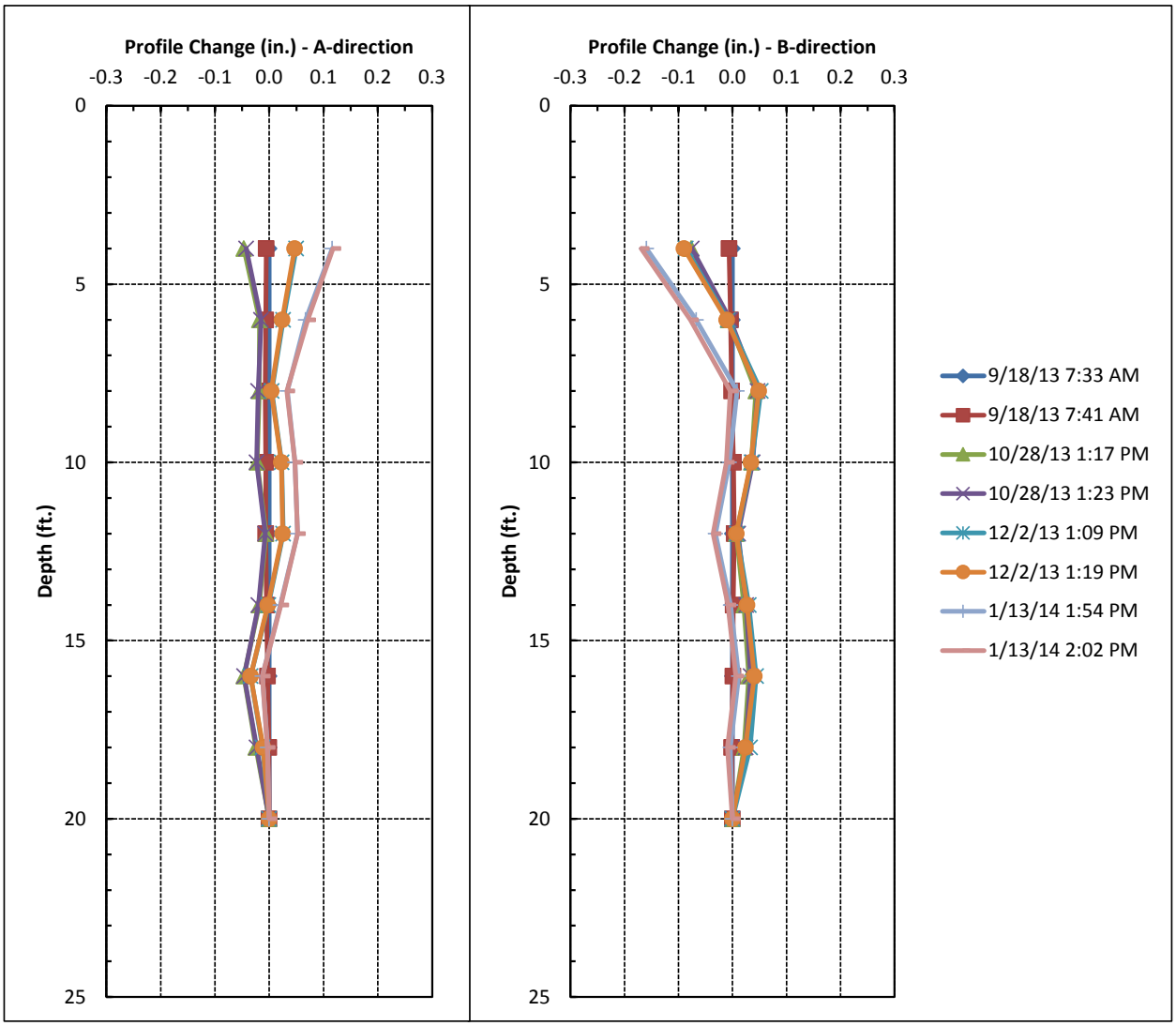

Figure 8. Inclinometer #1 in slope in McCurtain County (data above 4' was clipped due to erratic readings possibly due to casing installation).

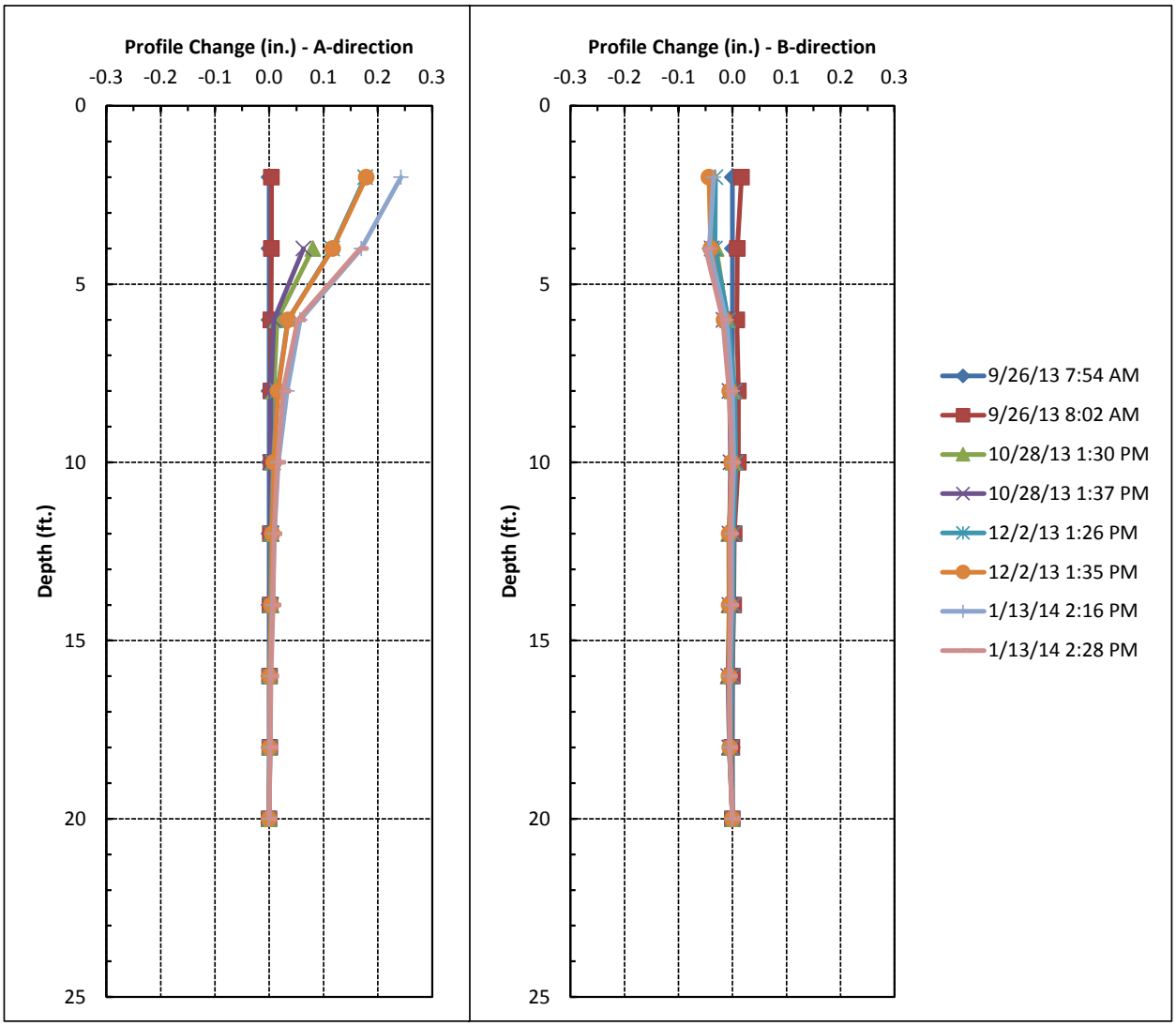

Figure 9. Inclinometer #2 in slope in McCurtain County (data above 2' was clipped due to erratic readings possibly due to casing installation).

The movement of the slope over the instrumentation period has been minimal; however, there was not a major rain event in those few months to trigger more movement. These inclinometers will be monitored monthly to see if and when there are any large slope movements and these will be correlated with the weather data. The data collected from this in situ monitoring instrumentation was used in the SLIDE model to attempt to predict, and then validate, slope failure.

Figure 10. Weather Station Installation on the Slope.

Task C2: Implement and Verify the Landslide Prediction Models

Empirical models (e.g., WLC) provide little theoretical basis for understanding how landslides might respond to hydrological processes; whereas physically based models consider the physical mechanisms influencing slope stability to assess landslide hazard, using a range of topographic, geologic, and hydrologic parameters. We further adopted the physically-based OU SLIDE (SLope-Infiltration Distributed Equilibrium) model (Liao et al., 2012) to evaluate model performance to see its potential as an effective prediction tool. Specifically, sensitivity tests at the Idabel site were conducted to investigate the impact of hydrological and geological properties on landslide modeling results.

Landslide model description

The physical model **SL**ope-**I**nfiltration **D**istributed **E**quilibrium (**SLIDE**) takes into account some simplified hypothesizes on water infiltration and defines a direct relationship between factor of safety (FS) and the rainfall depth on an infinite slope (Figure 11). This prototype model can provide landslide mapping and forecasting through the utilization of remote sensed and in situ surface data at larger scales. SLIDE has been applied and tested in Honduras during Hurricane Mitch in 1998 and quantitatively evaluated using landslide inventory data compiled by the United States Geological Survey (USGS). The agreement between the SLIDE modeling results and landslide observations demonstrates good predictive skills. However, due to the limitation of obtaining detailed soil information, backward analysis methods were used to derive and adjust soil parameters, rather than in situ tests. Here, in Oklahoma, several parameters in SLIDE can be directly measured from the in-situ observations or derived from the geotechnical laboratory tests. We believe this provides the best way to test the performance of a model as well as to clarify what physical processes are not

well presented in the current model. Using detailed soil data from laboratory and in situ testing would also provide valuable hints for future model refinement.

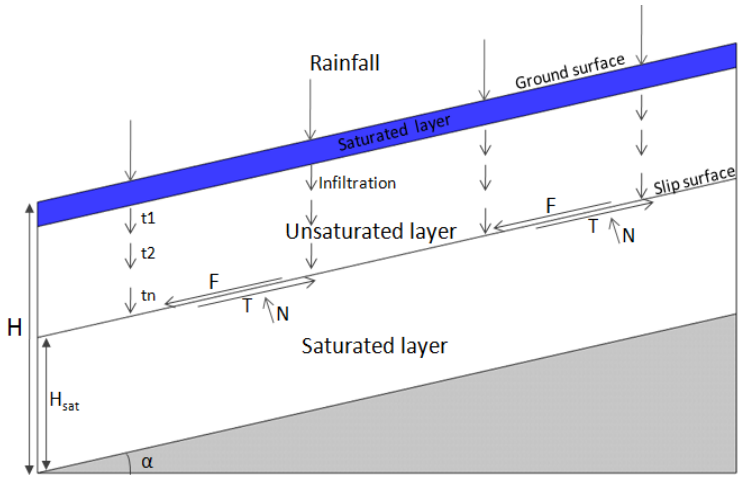

Figure 11. Schematic illustrating the SLIDE model of the infinite slope (adapted from Liao et al. (2012))

The SLIDE model integrates the contribution of apparent cohesion to the shear strength of the soil and soil depth influenced by infiltration processes. In Fig. 11, *N* is normal effective force, *T* is the shear force and t_i is the time step of infiltration. FS is expressed as the ratio of shear strength to shear stress to calculate slope stability. A slope is considered stable when FS>1 and a landslide is predicted when FS nears or drops below 1. SLIDE assumes that landslides occur in shallow depth and an infinite-slope equation is translated as the cohesion and frictional components:

$$FS(Z_t,t)=\frac{c'+c_\phi(t)}{\gamma_s Z_t \sin\alpha\cos\alpha}+\frac{\tan\varphi}{\tan\alpha} \quad (1)$$

where c' is soil cohesion, incorporating a value for root zone cohesion, γ_s is the unit weight of soil, α is slope angle and φ is soil friction angle. $c_\phi(t)$ represents the apparent cohesion related to matric suction, which in turn, depends on the degree of saturation of the soil (Montrasio and Valentino 2008), written as:

$$c_\phi(t)=A\cdot S_r\cdot(1-S_r)^\lambda\cdot(1-m_t)^\partial \quad (2)$$

where A is a parameter depending on the kind of soil and is linked to the peak shear stress at failure, λ and ∂ are numerical parameters which allow estimation of the peak of apparent cohesion related to S_r, the degree of saturation of the soil. m_t represents the dimensionless thickness of the infiltrated layer, which is a fractional parameter between 0 and 1:

$$m_t = \frac{\sum_{t=1}^{T} I_t}{n \cdot Z_t \cdot (1 - S_r)} \quad (3)$$

in which I_t is rain intensity, n is the porosity and Z_t is the soil depth at time t, which is determined by the infiltration processes:

$$Z_t = \sqrt{\frac{2 \cdot K_s \cdot H_c \cdot t}{\theta_n - \theta_0}} \quad (4)$$

where K_s is saturated hydraulic conductivity, H_c is capillary pressure, t is time, θ_n is water content of the saturated soil, and θ_0 is initial water content of the soil.

Study area and parameters

The location of the slope failure site is west of Idabel (33.49ºN, 94.52ºW), Oklahoma in a reconstruction project of the westbound lanes of US-70 in McCurtain County by the Oklahoma Department of Transportation (ODOT). At an elevation of 360ft above sea level, the slope has an average inclination of 30º and is covered with grassland (Figure 12).

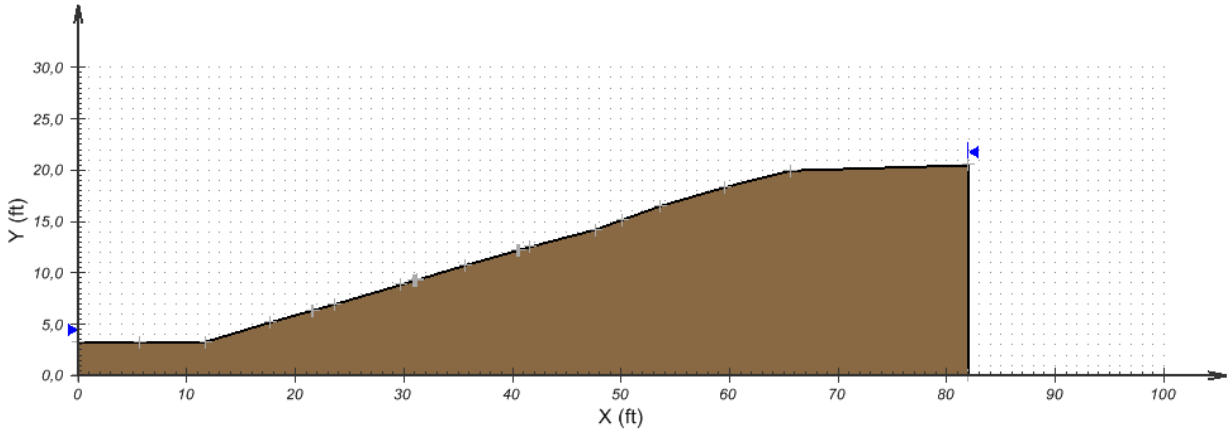

Figure 12. Slope Geometry (from Bourasset 2013).

In Idabel, an automatic hydrological monitoring system was installed in year October 2012, with a high temporal resolution (5-min) observation of rainfall, solar energy, wind, temperature, humidity and volumetric water content at three various depths (1ft, 3ft and 6ft). This study benefits greatly from very high quality one-year site-based in-situ measurements for the model evaluation.

The application of the SLIDE model requires the assignments of 14 parameters, as summarized in Tab. 5. Since the parameters have a large influence on SLIDE's

performance, it is imperative to assign values as realistic as possible based on field surveys and laboratory tests. Based on the findings in Cerato et al. (2007), some of the parameters can be derived, such as slope angle, friction angle, soil type and land cover. Other parameters were obtained from either the in situ monitoring, according to Liao et al. (2012) or based on other existing datasets (e.g., Food and Agriculture Organization (FAO) of the United Nations for soil properties).

Table 5. Parameters, symbols, and values used in SLIDE model at Idabel site

Property	Symbol	Unit	Value	Source
Slope angle	α	Deg	30	Field survey
Soil depth	Z_t	m [L]	Varies	Equation (4)
Soil type	/	Unit less	Stiff clay	Field survey
Land Cover	/	Unit less	Grassland	Field survey
Coefficients	λ, ∂	Unit less	0.4, 3.4	Liao et al. (2012)
Friction	φ	Deg	14.5	Cerato et al. (2007)
Cohesion (root included)	c'	KPa [M/LT^2]	41	FAO
Coefficient	A	KPa [M/LT^2]	20	Liao et al. (2012)
Unit weight of soil	λ_s	KN/m^3 [M/L^{2}T^2]	20	FAO
Porosity	n	1	0.47	FAO
Water content	θ	1	0.5, 0.9	Weather station
Degree of saturation	S_r	1	0.2	Liao et al. (2012)
Hydrologic conductivity	K_s	m/s [L/T]	8.83*10^{-5}	Liao et al. (2012)
Capillary	H_c	m [L]	0.05	Liao et al. (2012)

Results and discussion

In Idabel, we chose the representative rainfall event (R1) which happened from 2:30 a.m. to 6:15 a.m. on Mar 30, 2013. The highest recorded rainfall intensity of R1 was 8 mm/h, with an accumulation close to 15 mm in about 4 hours (Fig. 13, lower panel). However, according to SLIDE model, this rainfall event will not cause any landslide, as we can see from the top panel that the factor of safety within the entire time step is always larger than 1. We know from field surveys that the slope did not move, and so the SLIDE model predicted correctly that, with that particular rainfall event, the slope would not move.

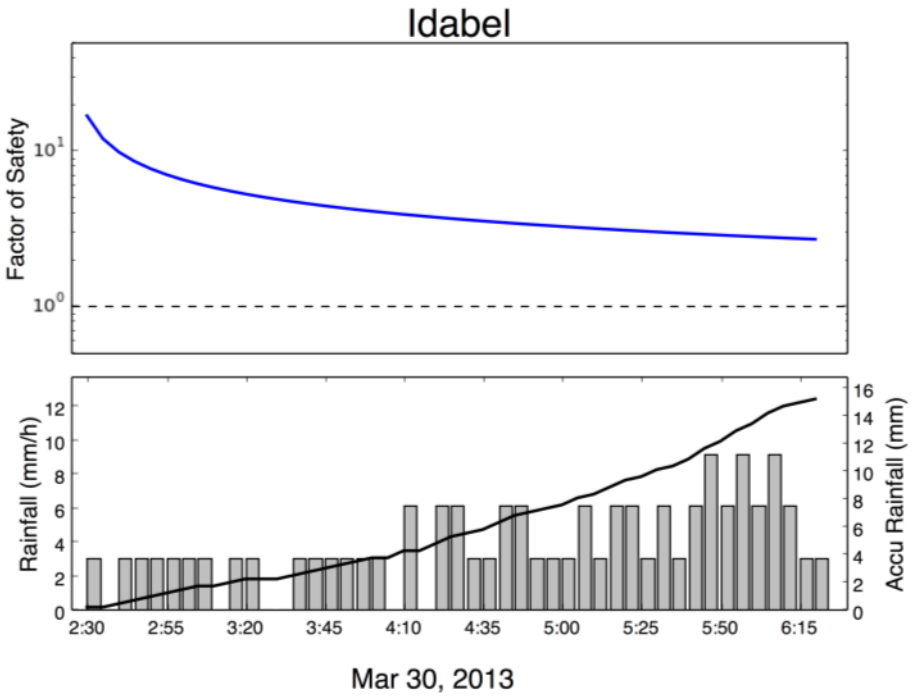

Figure 13. Measured instantaneous and accumulated rainfall and trend of the FS as a function of time in Idabel

Sensitivity analysis

The sensitivity of SLIDE was further investigated for different soil types. The purpose of this analysis was to find out what kind of soil would be more susceptible to landslides in the physical modeling. This could provide very useful information for choosing the location for the future construction of roadways along slopes. 12 of 16 soil types were chosen based on the classification in the FAO dataset. The main differences among these soil types reflected in SLIDE include soil cohesion, friction angle, porosity and saturated hydraulic conductivity. Tab. 6 shows the values used for the sensitivity analysis. Other parameters in SLIDE were kept the same. Results are represented in Fig. 14. FS drops below 1 in sand, loamy sand or sandy loam, which have a higher sand fraction, and lower clay fraction (e.g., lower cohesion). Soils with higher clay fractions, however, were not susceptible to rainfall triggered landslides in the SLIDE model. This can be explained according to Equation (1), in which soil cohesion plays an important role in determining the FS. The higher the soil cohesion is, the stronger resistance the soil column can provide, and therefore the more stable the slope is. While that makes sense in terms of the SLIDE model, and the use of cohesion (e.g., cohesion makes up the majority of the strength in bearing capacity equations for shallow foundations), we know that most of the landslides in Oklahoma occur in very clayey soils. This necessitates some modification to the existing model to better match the behavior of clay slopes in the field.

The sensitivity of the model to 'input forcing' (rainfall) and other geotechnical parameters was also evaluated (Fig. 15).

Table 6. Parameters for 12 soil types used for sensitivity analysis

Soil type	Soil cohesion (KPa)	Friction angle (degree)	Porosity	Saturated conductivity (m/s)
Sand	0	40	0.43	0.0011
Loamy sand	2	35	0.42	$3.02*10^{-4}$
Sandy loam	4	31	0.4	$1.46*10^{-4}$
Silt loam	6	29	0.46	$1.10*10^{-4}$
Silt	8	27	0.52	$2.39*10^{-4}$
Loam	28	24	0.43	$5.47*10^{-5}$
Sandy clay loam	27	21	0.39	$6.67*10^{-5}$
Silty clay loam	28	21	0.48	$1.27*10^{-4}$
Clay loam	29	19	0.46	$4.92*10^{-5}$
Sandy clay	30	17	0.41	$3.31*10^{-5}$
Silty clay	35	17	0.49	$8.20*10^{-5}$
Clay	40	17	0.47	$8.83*10^{-5}$

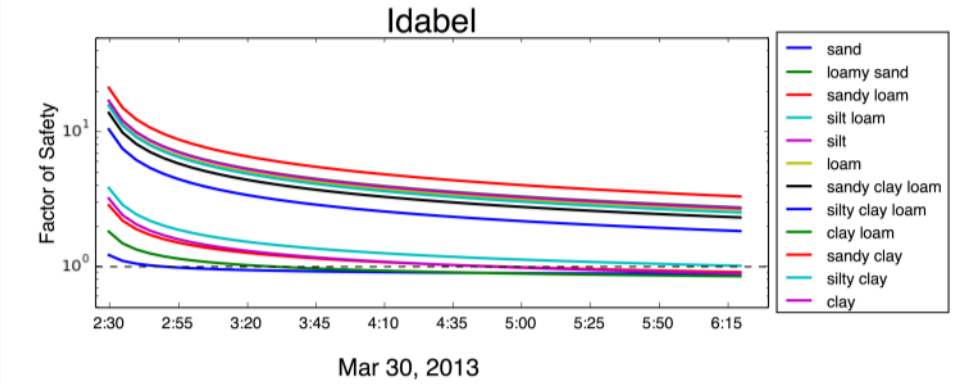

Figure 14. Temporal variation of the FS for 12 soil types in Idabel site

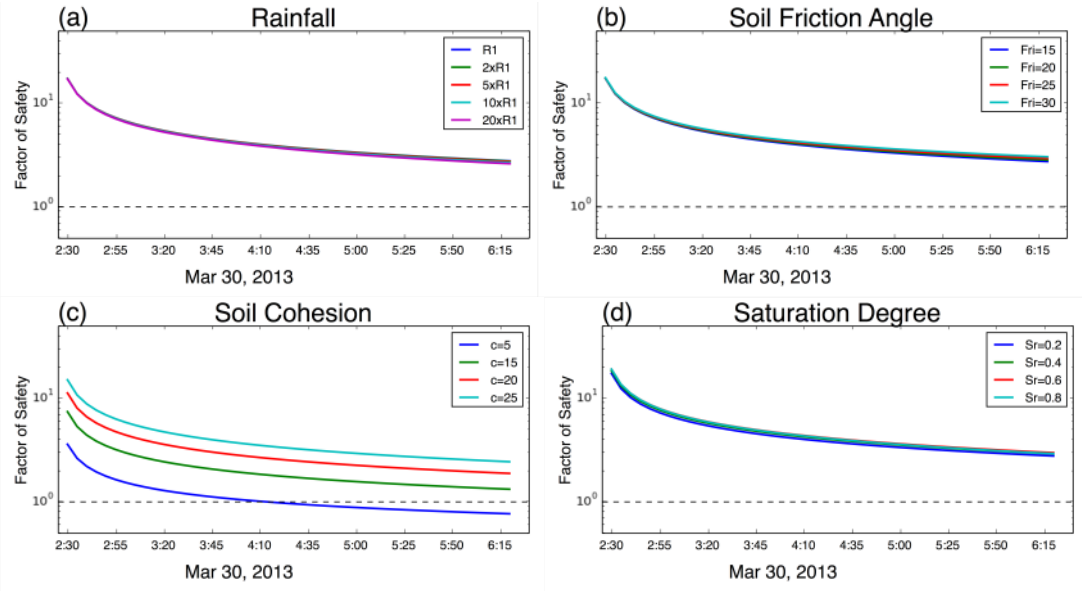

Figure 15. Sensitivity of the FS to different (a) rainfall scenario; (b) soil friction angle; (c) soil cohesion; (d) saturation degree

The geotechnical parameters considered in this study include soil friction angle, soil cohesion and degree of saturation. Only one parameter was changed in each run and the remaining parameters were kept at constant values. Fig. 15 (b) shows time series of the FS for different values of soil friction angle. As expected, slopes with higher friction angle (ϕ=30) and cohesion (c=25) have higher FS values than soils with low friction angle (ϕ=15) and cohesion (c=5), which means these slopes are more stable. The influence of degree of saturation (S_r) on FS is a little more complicated. As S_r increases, the FS will first increase and then decrease. This is because FS does not have a direct linear relationship with S_r. S_r controls both apparent cohesion ($c_\phi(t)$) and the dimensionless thickness of the infiltrated layer (m_t). In general, FS is not as sensitive to the soil friction angle or degree of saturation as soil cohesion. This indicates that soil cohesion plays a much more important role in determining the stability of slope compared to other parameters based on the current model framework. This is not surprising because higher soil cohesion would provide higher shearing resistance and therefore keep the slope more stable. This parameter is therefore an important parameter for model calibration.

It was surprising that model results were not more sensitive to the rainfall scenario; rainfall events are typically the "trigger" for landslides to occur. One reason that rainfall may not have that much of an effect in the current SLIDE model may be because it only has a direct influence on m_t (Equation 3) and an indirect influence on $c_\phi(t)$ (Equation 2). In order for it to have a more pronounced effect, it needs to play a bigger role in the SLIDE model, as cohesion does, which will require major modifications based on actual landslide events. Even with a much higher rainfall scenario, it is possible that $c_\phi(t)$ is not sensitive to the change of m_t given specific parameter combinations. Since default parameters based on Liao et al. (2012) were used in the model, further analysis will be

needed using landslide inventory datasets to calibrate the model in order to get better parameterization.

Failure soil depth

Due to the simplicity of the SLIDE model, a relationship between failure soil depth and cumulative rainfall can be derived according to Equation (1), (2) and (3). The failure soil depth Z_t at which the condition $F_s \leq 1$ is obtained is designed as the critical failure soil depth. It can be acquired by solving the following Equation using Mathematica software:

$$A \cdot S_r \cdot (1 - S_r)^{\lambda} \cdot (1 - \frac{cumRain}{n \cdot Z_t \cdot (1 - S_r)})^{\partial} = (\tan\alpha - \tan\varphi) \cdot \gamma_s \cdot Z_t \cdot \cos^2\alpha - c' \qquad (5)$$

The failure soil depth provides very useful information to estimate the total volume of the detached material, if the displacement of landslide can be measured or estimated. Figure 16 illustrates the relationship between failure soil depth and slope angle under different cumulative rainfall conditions. From the figure, we can see that as slope angle increases, failure soil depth decreases quickly. This indicates that at a steeper slope, a shallow landslide (2~4 m) is much more easily induced by the rainfall; while for a relatively shallow slope, the landslide would be a deep landslide (>6m). The latter case contradicts the model's hypothesis, which assumes that landslides occur at shallow depths. This points out another way in which the SLIDE model should be improved.

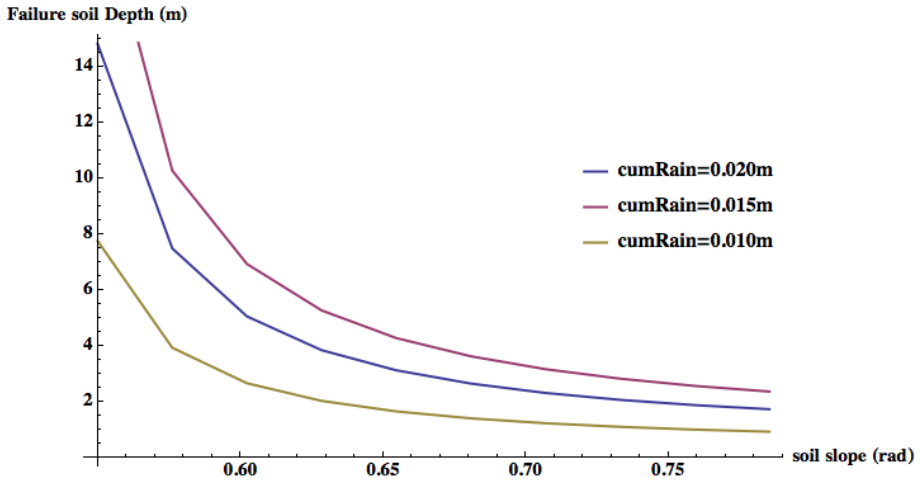

Figure 16. Relationship between failure soil depth and soil slope with different cumulative rainfall.

Limitations of the SLIDE model

Improvements and efforts related to this study can be extended focusing on the following aspects. First of all, SLIDE made several simple assumptions in order to make it easily applicable over large areas by employing various remotely sensed data sets. These assumptions may have significant effects on the simulation results. For example, SLIDE assumes all the rainfall infiltrates into the soil, neglecting run-off,

evapotranspiration and river routing. However, this assumption is not physically realistic. Further improvement would require us to couple the SLIDE model with a hydrological model, which can therefore better represent water balance and soil moisture dynamics.

Secondly, SLIDE model assumes soil depth has the linear relationship with $\sqrt{t}$. This is only applicable for the horizontal infiltration case or vertical infiltration but with very short time scales. In the future, we may consider using Green-Ampt infiltration model, which is more appropriate for vertical infiltration over relatively longer time scales.

Further more, the antecedent soil moisture conditions and groundwater pressure head are not incorporated in current model when calculating FS. This may cause biases when predicting the shear strength of soil at unsaturated conditions. It is therefore necessary to include more detailed modules, which account for the soil moisture in the unsaturated zone and water table dynamics. The SLIDE model overuses cohesion and downplays the importance of rainfall in the model and that is why the predictions of the clayey Idabel site show very little possibility for failure, even though we know there is sliding. Finally, the model ignores the presence of any desiccation cracks on the slope, which could have significant influence on the slope stability. Typically, the higher the cohesion, the higher the clay content in the soil, and so, the higher the chance to develop desiccation cracks when dry. Thus, during a rainfall event, a large quantity of the water will be able to infiltrate in these macro-cracks, even if the permeability of the soil is very low, resulting in a rapid increase in the weight and a sudden decrease in suction leading to a loss in shearing resistance.

Conclusions and Recommendations

During this project, 113 historic and current landslides were identified, mapped and analyzed across the state. The ODOT Division engineers in Divisions 1, 2 and 3 provided 23 locations and the USGS provided 80. Soil information from the United States Department of Agriculture (USDA) Natural Resources Conservation Service (NRCS) was collected for all 113 sites, and more detailed soil information, including moisture contents, Atterberg Limits and Grain Size Distributions were collected for currently problematic landslides. In addition, all currently active landslides were mapped, if accessible, to determine the extent of the sliding. One landslide was chosen to further instrument with a weather station and inclinometers. In addition, advanced soil testing was performed, including triaxial and direct shear testing. This in situ and laboratory data was used as validation for the SLIDE model, used to predict landslides.

After establishing a comprehensive landslide database for Divisions 1, 2 and 3 (based on experiential knowledge of the landslide locations from the ODOT Division Engineers) a regional landslide map was created. This map better refines the problematic areas of the state and shows that slope, soil texture type, land cover have a large impact on the susceptibility of the site to slide, whereas, elevation had relatively no impact. Almost all of the landslide locations provided to us fell within the high and very high susceptibility ratings, which demonstrates the ability of GIS-based weighted linear combination models in predicting landslide hotspots.

One site in McCurtain County near Idabel along Route 70 was monitored for in situ moisture, temperature and rainfall, among other parameters, since October of 2012. Inclinometers, to measure the slope movement, were installed September of 2013. All the relevant data has been included in Appendix A. Obviously, pairing the weather station data with the inclinometer data over a wet-season would have helped to understand the slope movement and validate the SLIDE model more completely, but several important recommendations can still be made. The slope at Idabel consists of a fat clay, CH, with a PI of 46% and a uniformly high in situ moisture content throughout the depth of the slide mass around 25%. While the slope of this site is only 30%, or roughly 3:1, the geology (shallow limestone), and highly weathered Hollywood soil series, creates a perfect sliding scenario. When it rains, the clay absorbs the water, gets heavy, and slides. Mitigation in the area has included rock drains parallel with the slope in order to get the water out of the slope more quickly. If right-of-way (ROW) is available, it would also help to lay back the slope to even shallower angles when roadways are built or maintained through similar geology. The SLIDE model needs to be modified so that rainfall plays a much bigger role in predicting landslides, and that cohesion does not just act as a resisting force, but as an indicator to soil adsorption and loss of suction with rain infiltration. Throughout the following years, the in situ monitoring equipment will continue to be used to validate the model until it can predict a slide occurrence accurately.

References

Ayalew, L., H. Yamagishi, and N. Ugawa, 2004: Landslide susceptibility mapping using GIS-based weighted linear combination, the case in Tsugawa area of Agano River, Niigata Prefecure, Japan, Landslide 1:73-81

Anbalagan, R., 1992, Landslide hazard evaluation and zonation mapping in mountainous terrain. Engineering Geology 32: 269-277

Anderson, D.M. & Tice, A.R. 1972. Predicting Unfrozen Water Contents in Frozen Soils from Surface Area Measurements. Highway Research Record No. 393: 12-18.

Baum, R. L., W. Z. Savage, and J. W Godt, 2002: TRIGRS – A Fortran program for transient rainfall infiltration and grid-based regional slope-stability analysis: U. S. Geological Survey Open-File Report 02-0424, 64 p. http://pubs.usgs.gov/of/2002/ofr-

Bourasset, Celine. 2013. Investigation of Shear Strength and Stability of Shallow Slopes Under Changing Moisture Conditions. A MS Thesis presented to the University of Oklahoma in partial fulfillment of the requirement for the degree.

Brunauer, S., Emmett, P.H., and Teller, E., 1938. Adsorption of Gases in Multi-Molecular Layers. Journal of the American Chemical Society. (60) 309-319.

Cannon, S.H., J.E. Gartner, R. C. Wilson, and J.L. Laber (2008). "Storm rainfall conditions for floods and debris flows from recently burned areas in southwestern Colorado and southern California", Geomorphology, 96, 250-269.

Carrara, A., M. Cardinali, R. Detti, F. Guzzetti, V. Pasqui, and P. Reichenbach, 1991, GIS techniques and statistical models in evaluating landslide hazard. Earth Surface Processes and Landforms, 16, 427– 445

Cerato, A.B. and Lutenegger, A.J. 2002. Determination of Surface Area of Fine-Grained Soils by the Ethylene Glycol Monoethyl Ether (EGME) Method. *Geotechnical Testing Journal (GTJ), ASTM*. (25:3) 315-321.

Cerato, A.B. and Lutenegger, A.J. 2005. Activity, Relative Activity and Specific Surface Area of Fine-Grained Soils. Proceedings of the 16th International Conference on Soil Mechanics and Geotechnical Engineering (ICSMGE). Sept. 12-16, 2005, Osaka, Japan.

Cerato, A.B., Miller, G.A. and Hajjat, J. (2009). The Influence of Clod-Size and Structure on Wetting-Induced Volume Change of Compacted Soil. ASCE Journal of Geotechnical and Geoenvironmental Engineering. Vol. 135, No. 11, pp. 1620-1628.

Cerato, A.B. and Nevels, J.B. (2007). Shallow Landslide Analysis: McCurtain County, Oklahoma. Proceedings of the 1st North American Landslide Conference: Landslides and Society: Integrated Science, Engineering, Management, and Mitigation. Vail, CO, June 3-8, 2007, pp. 21-30.

Cerato, A.B., Oleski, R.C. and Puklin, C.C. (2006). Case Study: Compacted Embankment Landslide in Grady County, Oklahoma. Proceedings of the 40th Annual Symposium on Engineering Geology and Geotechnical Engineering. Landslides – Investigation, Analysis and Mitigation. Utah State University, Logan, Utah, May 24-26, 2006, CD Proceedings.

Coe, J. A., Godt, J. W., Baum, R. L., Bucknam, R. C., and Michael, J. A.: Landslide susceptibility from topography in Guatemala, in: Landslides: Evaluation and Stabilization, edited by: Lacerda, W. A., Ehrlich, M., Fontura, S. A. B., and Sayão, A.S. F., Taylor & Francis Group, London, 69 - 78, 2004.

Dai, F.C., Lee CF, 2002, Landslide characteristics and slope instability modeling Using GIS, Lantau Island, Hong Kong, Geomorphology 42:213–238.

Dasog, G.S., Acton, D.F., Mermut, A.R. & DeJong, E. 1988. Shrink-Swell Potential And Cracking in Clay Soils of Saskatchewan. Canadian Journal of Soil Science, Vol. 68:251-260.

Dietrich, W. E. and R.R. Asua (1998) "A validation study of the shallow slope stability model, SHALSTAB, in forested lands of Northern California" http://socrates.berkeley.edu/~geomorph/shalstab/index.htm

Dos Santos, M.P.P. & DeCastro, E. 1965. Soil Erosion in Roads. Proceedings of the 6th International Conference on Soil Mechanics and Foundation Engineering, Vol. 1: 116-118.

Fabbri, A. G., C.F. Chung, A. Cendrero, and J. Remondo, 2003, Is prediction of future landslides possible with GIS? Journal of Natural Hazards 30: 487-499.

Fan and Hsiao· 2010. Effect of Slope Terrain on Distribution of Matric Suction in Unsaturated Slopes Subjected to Rainfall. Experimental and Applied Modeling of Unsaturated Soils (GSP 202). Proceedings of the 2010 GeoShanghai International Conference

Fernandez, T., C. Irigaray, R. El Hamdouni, and J. Chacon, 2003: Methodology for Landslide Susceptibility Mapping by Means of a GIS, Application to the Contraviesa Area (Granada, Spain), Journal of Natural Hazards, 30, 297-308

Hong, Y., Adler, R., and Huffman, G.: Evaluation of the potential of NASA multi-satellite precipitation analysis in global landslide hazard assessment, Geophysical Research Letters, 33, L22402, 2006.

Hong, Y., Adler, R., and Huffman, G.: Use of Satellite Remote Sensing Data in the Mapping of Global Landslide Susceptibility, Journal of Natural Hazards, 43, 245-256, 2007a.

Hong, Y., Adler, R. F., and Huffman, G.: An Experimental Global Prediction System for Rainfall-Triggered Landslides Using Satellite Remote Sensing and Geospatial Datasets, IEEE Transactions on Geosciences and Remote Sensing, 45, 1671-1680, 2007b.

Hong, Y., Adler, R. F., and Huffman, G. J.: Satellite Remote Sensing for Landslide Monitoring on a Global Basis, American Geophysical Union EOS, 88, 357-358, 2007c.

Hong, Y and R.F. Adler, 2008, Predicting Landslide Spatiotemporal Distribution: Integrating Landslide Susceptibility Zoning Techniques and Real-time Satellite Rainfall, *Special Issue of International Journal of Sediment Research*, Vol. 23, No. 3, 2008, pp. 249–257.

Godt, J.W., R. L. Baum and N. Lu (2009) "Landsliding in partially saturated materials", Geophysical research letters, Vol. 36, L02403.

Guzzetti, F., A. Carrara, M. Cardinali, P. Reichenbach, 1999, Landslide hazard evaluation: a review of current techniques and their application in a multi-scale study, Central Italy. Geomorphology 31:181–216.

Iverson, R.M. (2000) "Landslide triggering by rain infiltration", Water Resources Research, v. 36, no. 7, p. 1897-1910.

Kim, Y.K. and Lee, S.R. (2010). Field Infiltration Characteristics of Natural Rainfall in Compacted Roadside Slopes. Journal of Geotechnical and GeoEnvironmental Engineering. Vol. 136, No. 1, pp. 248-252.

Larsen, M.C., and A. J. Torres Sanchez, 1998: The frequency and distribution of recent landslides in three montane tropical regions of Puerto Rico: Geomorphology, v. 24, p. 309-331.

Lee, S., K. Min (2001). Statistical analysis of landslide susceptibility at Yongin, Korea, Environ Geol 40:1095–1113.

Liao, Z., Y, Hong, J. Wang, H. Fukoka, K. Sassa, D. Karnawati, and F. Fathani, 2010: Prototyping an experimental early warning system for rainfall-induced landslides in Indonesia using satellite remote sensing and geospatial datasets. *ICL Landslides Journal,* Volume 7 Issue 3 page 317-324.

Liao Z, Hong Y, Kirschbaum D, Liu C (2012). Assessment of shallow landslides from Hurricane Mitch in central America using a physically based model. Environ Earth Sci, 66(6): 1697-1705.

Low, P.F. 1980. The Swelling of Clay: II. Montmorillonite. Soil Science Society of America Journal, Vol.44, No. 4: 667-676.

Metternicht, G, L. Hurni and R. Gogu (2005) "Remote sensing of landslides: an analysis of the potential contribution to geo-spatial systems for hazard assessment in mountainous environments", Remote Sens. Environ. 98 (2-3): 284-303.

Mitchell, J.K. 1976. Fundamentals of Soil Behavior. John Wiley & Sons, New York.

Morgenstern, N.R. & Balasubramanian, B.I. 1980. Effects of Pore Fluid on the Swelling of Clay-Shale. Proceedings of the 4th International Conference on

Expansive Soils, Vol. 1: 190-205.
Montrasio L ,Valentino R (2008) A model for triggering mechanisms of shallow landslides. Nat Hazards Earth Syst Sci 8:1149-1159.

Nixon, J.F. 1991. Discrete Ice Lens Theory for Frost Heave in Soils. Canadian Geotechnical Journal, Vol. 28: 843-859.

Oregon Transportation Research and Education Consortium (OTREC). Project # 2011- 398: Real-time change and damage detection of landslides and other earth movements threatening public infrastructure. PI. Michael J. Olsen, Assistant Professor, Oregon State University.

Pinilla, J.D., Miller, G.A., Cerato, A.B. and Snethen, D.S. (2011). Influence of Curing Time on the Resilient Modulus of Chemically Stabilized Soils. ASTM Geotechnical Testing Journal (GTJ). Vol. 34, No. 4. pp. 364-372.

Ray, R.L and J.M. Jacobs (2007, December) "Landslide forecasting using microwave remote sensing", Poster session presented at AGU Fall Meeting, San Francisco, CA.

Ray, R.L., Jacobs, J.M. and de Alba, P. (2010). Impacts of Unsaturated Zone Soil Moisture and Groundwater Table on Slope Instability. Journal of Geotechnical and GeoEnvironmental Engineering. Vol. 136, No. 10, pp. 1448-1458.

Restrepo, P., D.P. Jorgensen, and S.H. Cannon, et al. (2008) "Joint NOAA/NWS/USGS Prototype Debris Flow Warning System for Recently Burned Areas in Southern California", Submitted to the Bulletin of the American Meteorological Society.

Rhoades, J.D. 1982. Cation Exchange Capacity. Methods of Soil Analysis, Part 2, Second Edition. Agronomy Monograph 9, American Society of Agronomy, Madison, WI.

Rieke, R.D., Vinson, T.S. & Mageau, D.W. 1983. The Role of Specific Surface Area and Related Index Properties in the Frost Heave Susceptibility of Soils. Proceedings of the 4th International Permafrost Conference: 1066-1071.

Ross, G.J. 1978. Relationships of Specific Surface Area and Clay Content to Shrink- Swell Potential of Soils Having Different Clay Mineralogic Compositions. Canadian Journal of Soil Science, Vol. 58: 159-166.

Saha, A. K., R.P. Gupta, and M.K. Arora, 2002: GIS-based landslide hazard zonation in the Bagirathi (Ganga) Valley, Himalayas, International Journal of Remote Sensing, 23, no.2, 357-369. 2002

Sarkar, S., D. P. Kanungo (2004): An integrated approach for landslide susceptibility mapping using remote sensing and GIS. Photo Eng Remote Sens 70:617–625

Sidle, R.C. and H. Ochiai, 2006, Landslide Processes, Prediction, and Land use, Washington DC, American Geophysical Union, pp1-312.

Texas Department of Transportation Geotechnical Engineering Manual. Chapter 7: Slope Stability.

Trauner, F-X, Boley, C. and Nuhn, E. (2010). Identification of landslide susceptible slopes and risk assessment using a coupled GIS-FEA-module. Proceedings of the 2010 GeoShanghai International Conference, Geotechnical Special Publication No. 206. Page 120-125.

Zhang, Z., Cui, W. and Guo, R. (2010). Effect of Environmental Conditions on Stability of an Unsaturated Soil Slope. Proceedings of the 2010 GeoShanghai International Conference. Geotechnical Special Publication No. 206. Part II: Applied Modeling and Analysis. Page 144-151.

Appendix A – Soil Data from Instrumented Slide in Idabel

Table_APX_A 1. Basic Properties of Idabel Soil.

Liquid Limit (%)	72
Plastic Limit (%)	26
Plasticity Index (%)	46
Specific Gravity	2.78
Sand (%)	3.5
Silt (%)	16.9
Clay (%)	79.6
Maximum Dry Unit Weight (pcf)	96.8
Optimum Moisture Content (%)	24

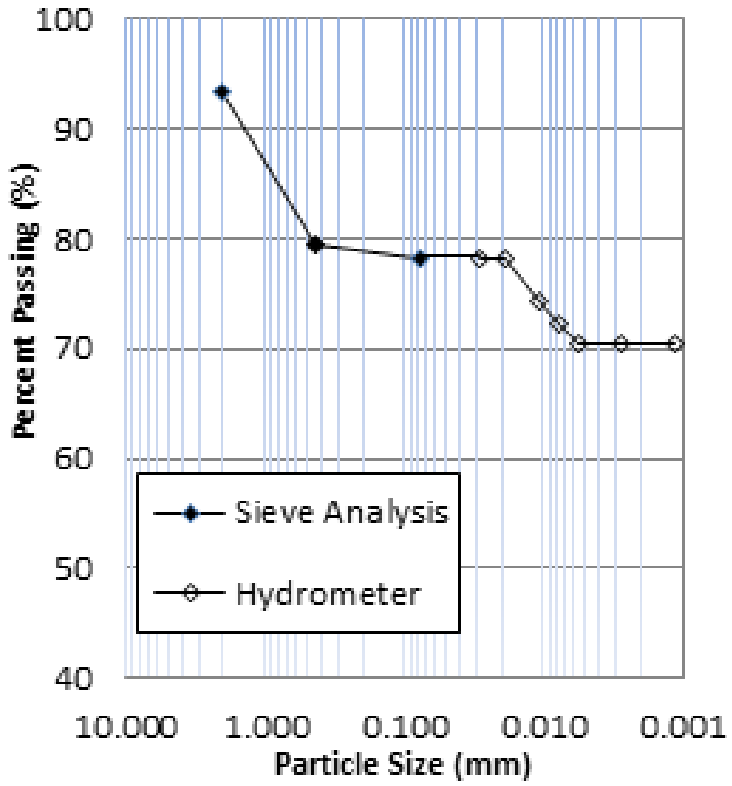

Figure_APX_A 1. Grain Size Analysis from Idabel (from Bourasset 2013).

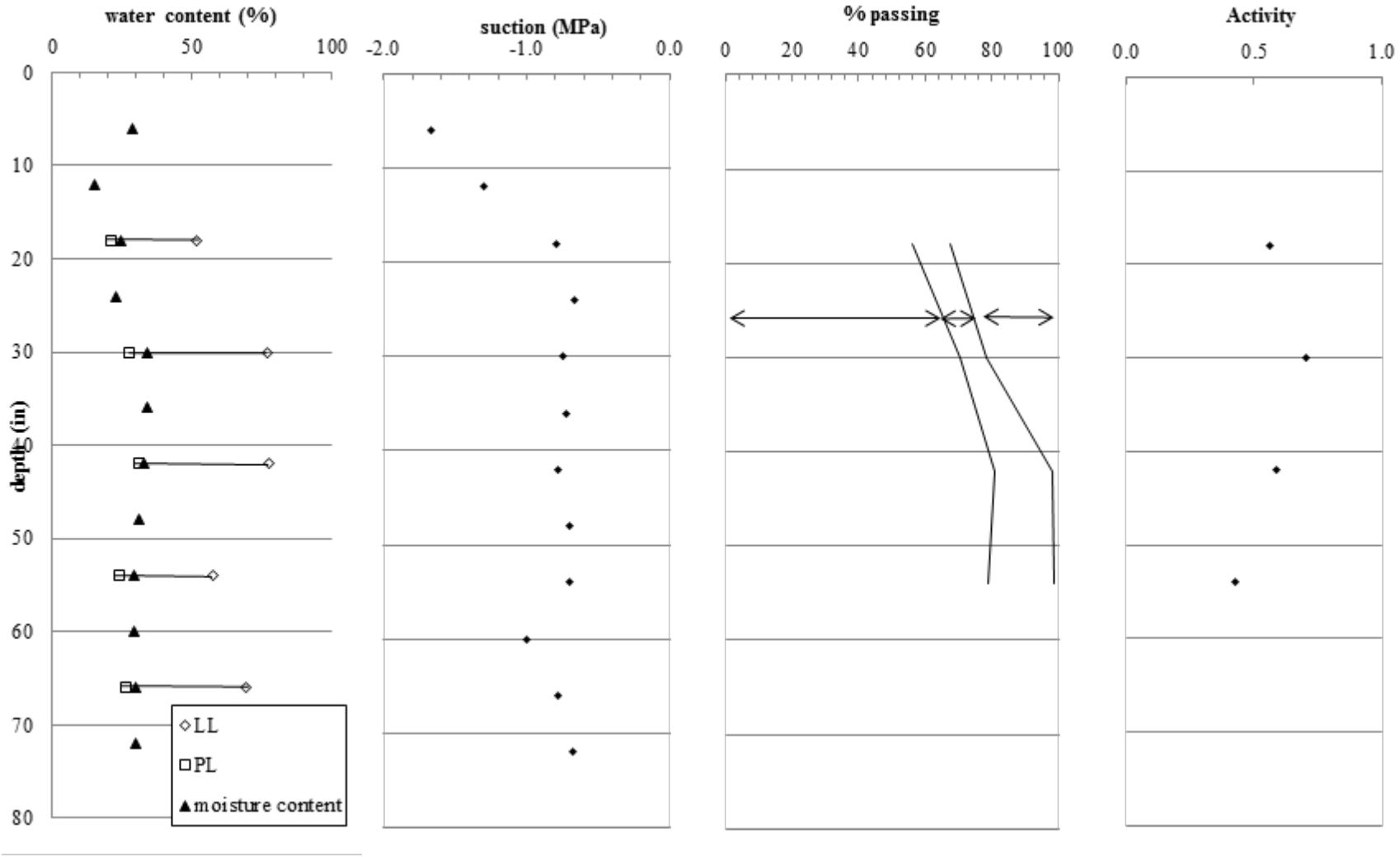

Figure_APX_A 2. Idabel Soil Profile (from Bourasset 2013)

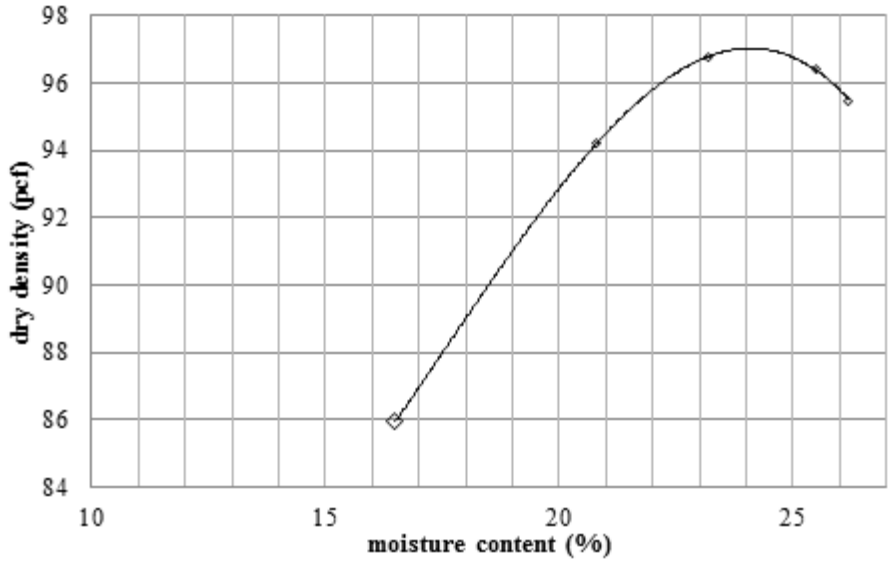

Figure_APX_A 3. Standard Proctor Curve for Idabel. (from Bourasset 2013)

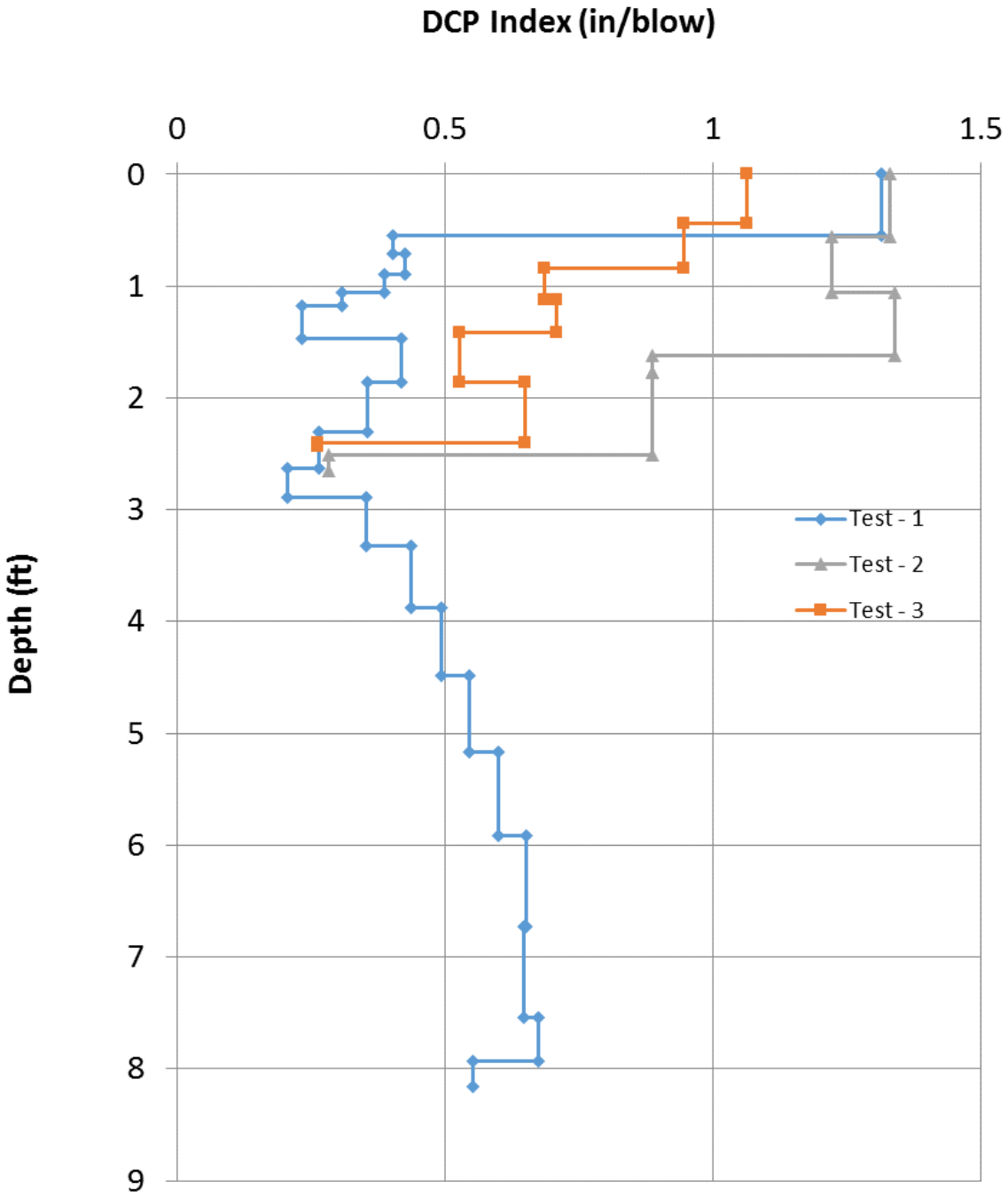

Figure_APX_A 4. Dynamic Cone Penetration Test Profile.

Triaxial Strength Data

Table_APX_A 2. Idabel site, summary of triaxial test results (from Bourasset 2013)

depth (in)	avg depth (in)	dry density (pcf)	water content (%)	Φ' (°)	Su/Po
17 -23	20	91.79	26.3	28.8	0.45
24 - 31	27	88.67	25.7	29.4	0.37
33 -39	36	90.54	29.2	27.6	0.37
38 - 45	41	101.78	16.5	18.6	0.61
37 - 49	43	101.78	21.2	24.9	0.34

From these plots, a change of shear strength can be observed with an important decrease of the friction angle. The decrease in average friction angle below 30 inches is likely due to the increase in average PI below 30 inches as seen in Figure A5. It can be seen that the undrained shear strength increases as the depth increases.

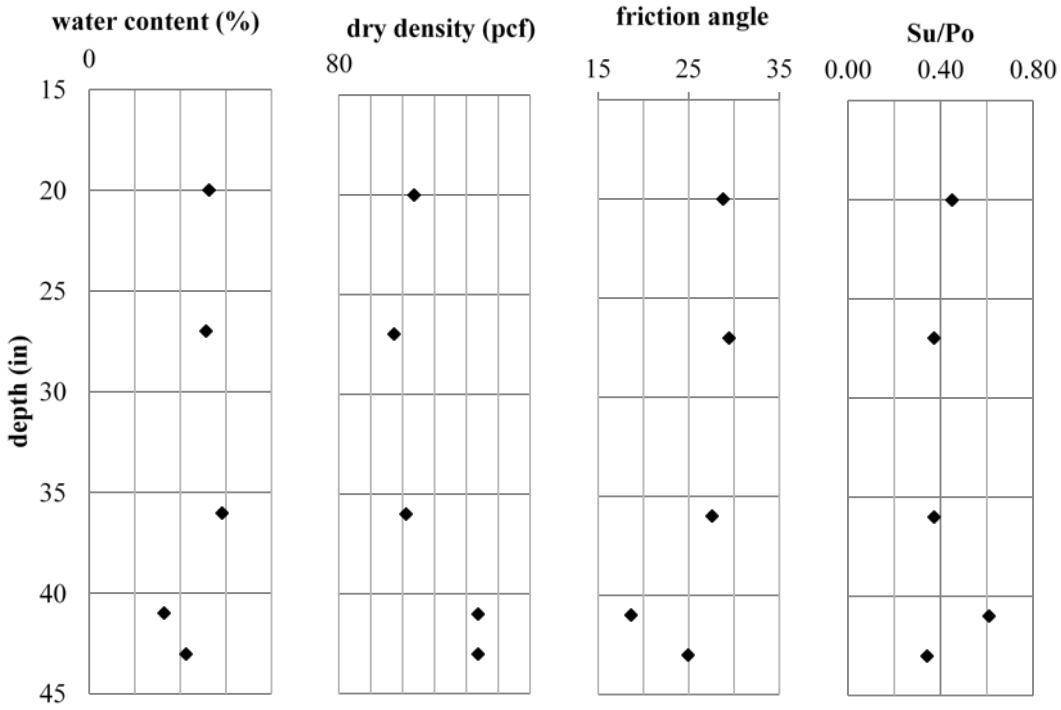

Figure_APX_A 5. Summary of Triaxial Results (from Bourasset 2013)

When looking at the failure envelopes from the different tests (Figure A6), it is noticed that they are slightly curved, with higher friction angle at lower normal stresses. As the

slip failure is assumed to be shallow, we were focusing on the first part of the curve. Considering only the lower range of effective stresses of the curve instead of taking an average, higher values of friction angle were used to define the shear strength of the soil.

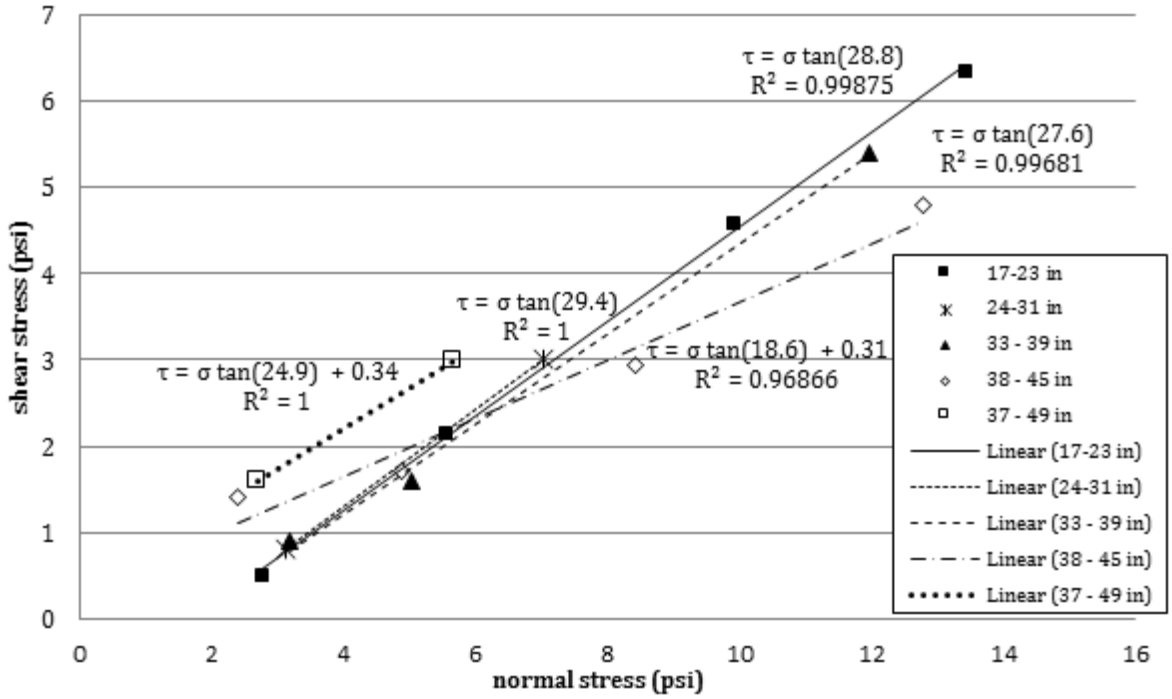

Figure_APX_A 6. Summary of Triaxial Results (from Bourasset 2013)

Direct Shear Testing

Samples were subjected to cycles of 24-hour wetting then 24-hour drying and their height and weight were recorded at the end of each cycle. As the Idabel soil is a highly plastic soil, important changes in volume were observed. The soil shrunk and cracked during the drying period and swelled during wetting to close the cracks that appeared when the sample was dry. Figures A7 and A8 show a sample after a drying period and a wetting period, respectively.

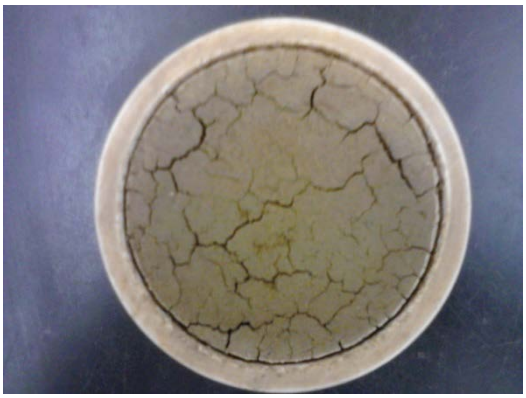

Figure_APX_A 7: specimen after drying

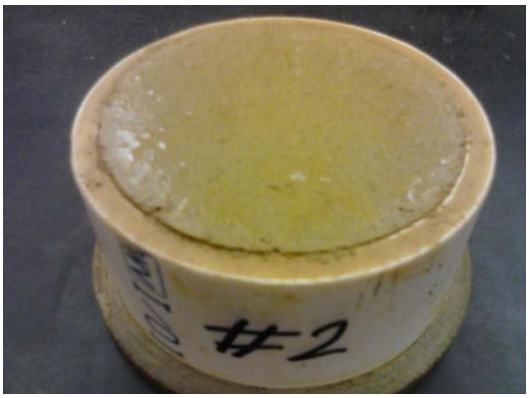

Figure_APX_A 8: specimen after wetting

The change in moisture content and dry density is shown in Figures A9 and A10 for the Idabel Sample 1.In these Figures, it can be seen that the moisture content and the dry density vary at the beginning but then reach some equilibrium value and stabilize after the 7th cycle (i.e., after 2 weeks). Some soil was lost during the handling of the specimens but the amount lost is too small to explain the variation that is observed at the beginning.

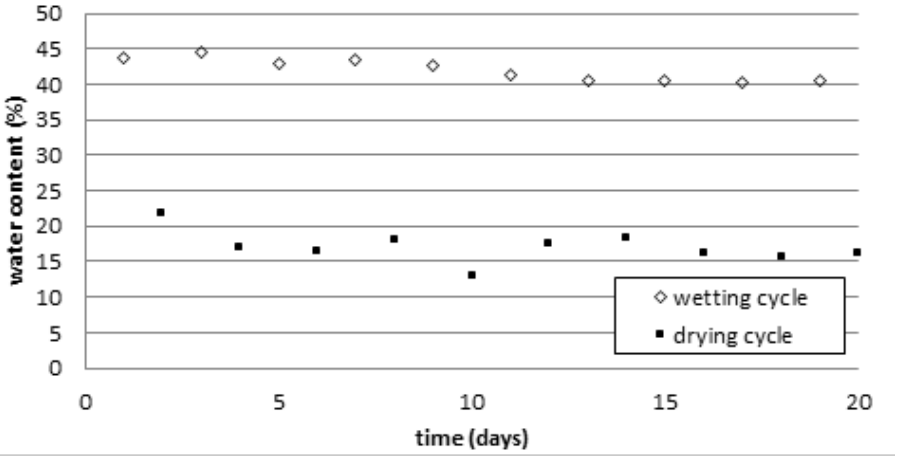

Figure_APX_A 9. Evolution of moisture content over wetting and drying cycles (from Bourasset 2013).

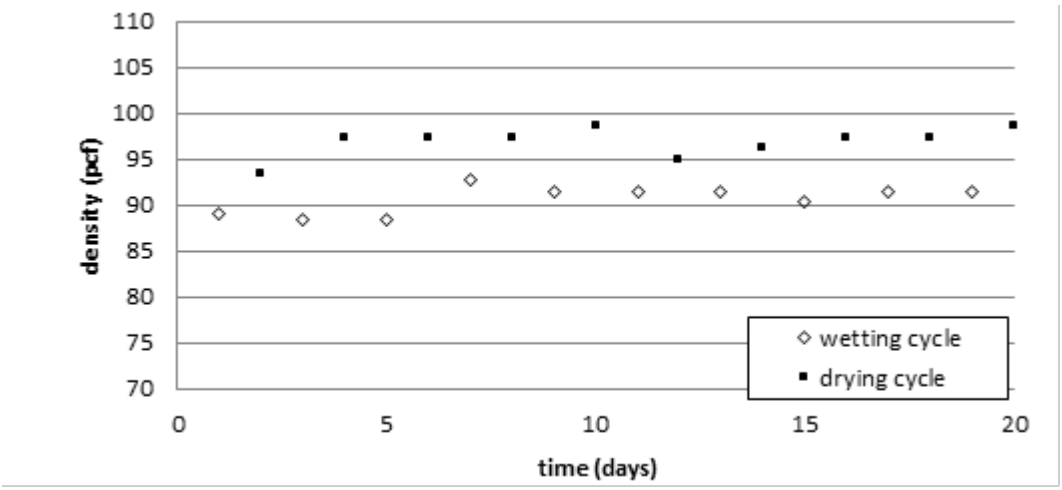

Figure_APX_A 10. Evolution of dry density over wetting and drying cycles (from Bourasset 2013).

Samples were actually subjected to 10 cycles of wetting and drying plus one cycle of wetting as the sample had to be wet to be trimmed for testing. The results of two typical direct shear tests for samples subjected to cycles of wetting and drying for a normal stress of 2 and 5 psi are shown in Figure A11. For these tests, the maximum shear stress observed during shearing was used to determine the fully softened strength.

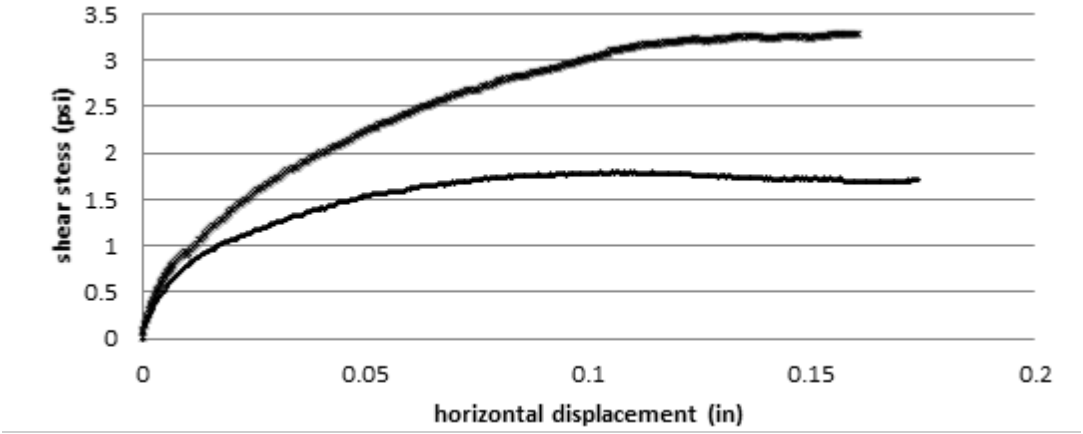

Figure_APX_A 11. Direct shear tests conducted under 2 and 5psi normal stress (from Bourasset 2013).

.

Figure A12 shows the results obtained from the direct shear tests. The slope of the failure envelope gives a friction angle of 25.2°. A cohesion intercept of 0.9psi was found, considering the failure envelope as being a straight line.

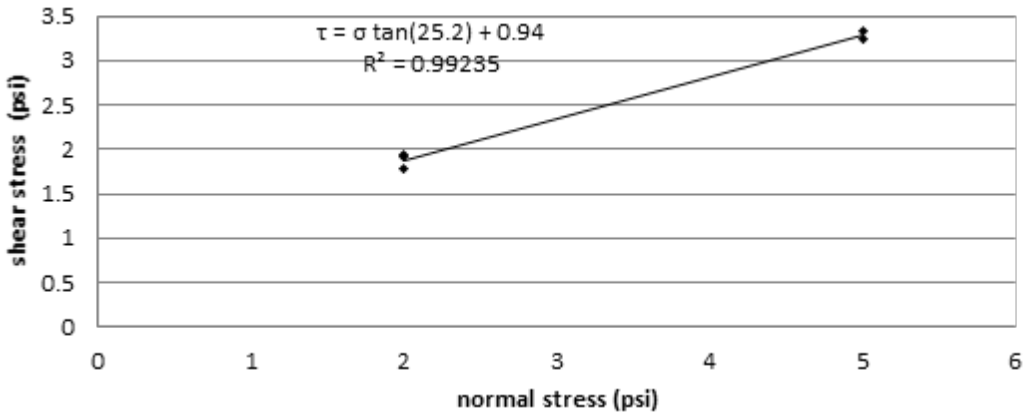

Figure_APX_A 12. Direct shear tests results on Idabel samples subjected to wetting and drying cycles (from Bourasset 2013).

The specimens, compacted at the same water content and dry density as the specimens subjected to cycles of wetting and drying, exhibit a peak strength and then a decrease in the strength until a post peak strength is reached. Figure A13 summarizes the results of the direct shear tests on recreated samples and shows the difference between the peak strength envelope and the post-peak strength envelope.

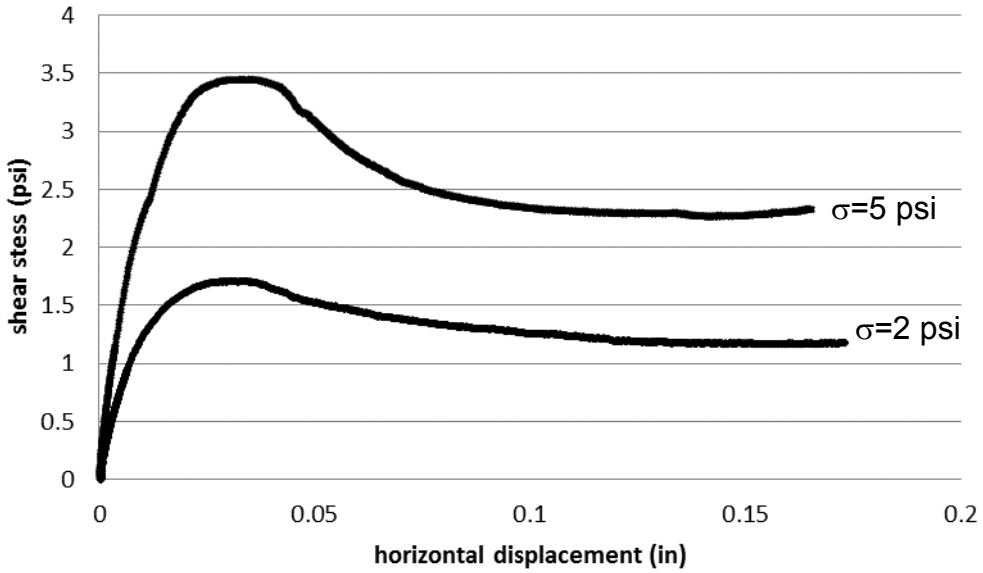

Figure_APX_A 13. Strength evolution for samples sheared under 2 and 5 psi confining pressure (from Bourasset 2013).

The failure envelope in Figure A14 gives a friction angle equal to 23.4° and a cohesion of 1psi for the peak strength. The post-peak failure envelope gives a friction angle equal to 15.2 and a cohesion of 0.82psi. The cohesion for normally consolidated

specimens is expected to be zero; which may not be the case here because of residual bonds between the particles (from the overconsolidated state).

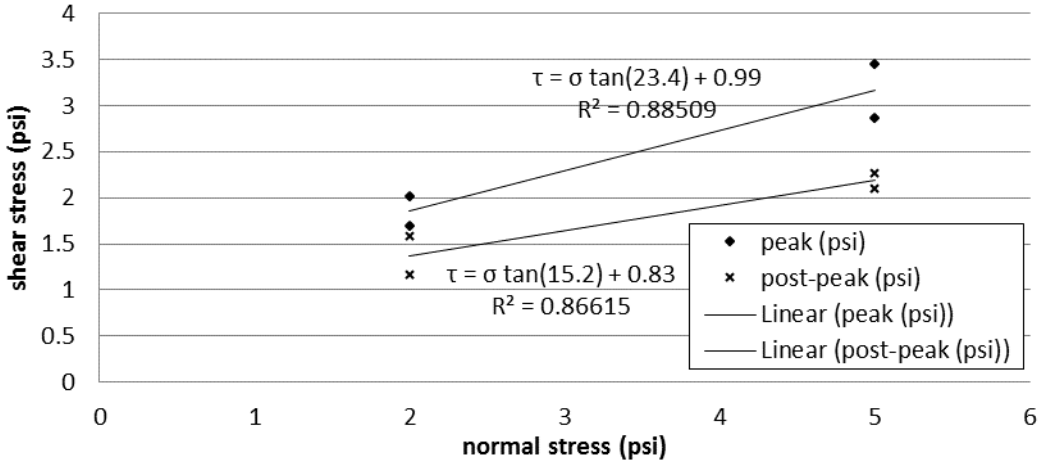

Figure_APX_A 14. Results of direct shear tests on specimens recreating softened conditions for Idabel soil, peak and post peak strength (from Bourasset 2013).

Figure A15 shows the results (peak strength) obtained from direct shear tests conducted on specimens subjected to cycles of wetting and drying and on specimens recreating the softened state (i.e., same dry density and moisture content). Both procedures resulted in a similar fully softened failure envelope.

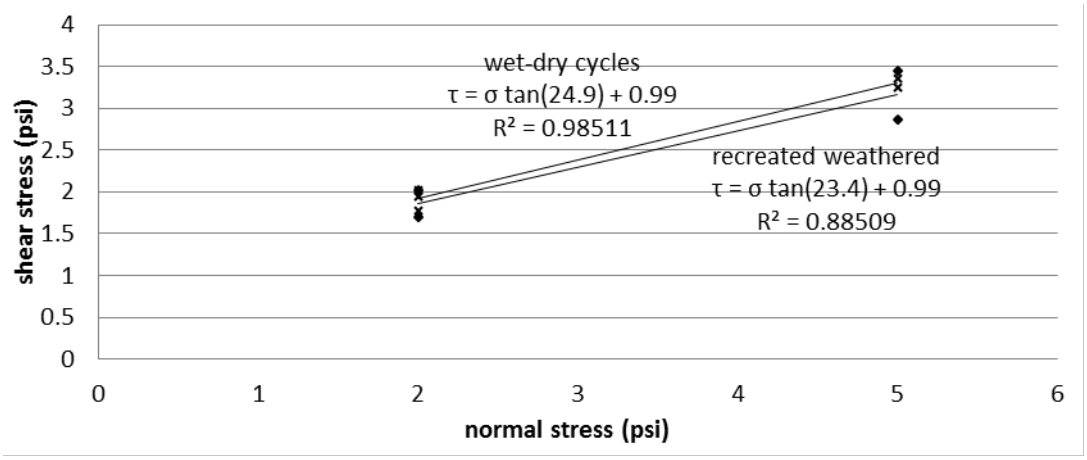

Figure_APX_A 15. Comparison of failure envelopes between samples subjected to cycles of wetting and drying and samples recreating the final conditions (from Bourasset 2013)

It is important to note that even if the failure envelope is similar, the samples from cyclic wetting and drying and those recreating the same final conditions (but not subjected to these cycles) did not behave the same way during shearing. Indeed, the samples subjecting to cycles of wetting and drying exhibit the behavior of normally consolidated clay while the samples recreating the softened conditions act like over-consolidated clays. As can be seen in Figure A16, after a certain displacement both

specimens reached a post peak shear stress corresponding to different values. The difference between these values seems to increase as the normal stress increases. As shown in Figure A16, for the case of artificially weathered samples the soil contracts; whereas it dilates for the samples recreating softened conditions.

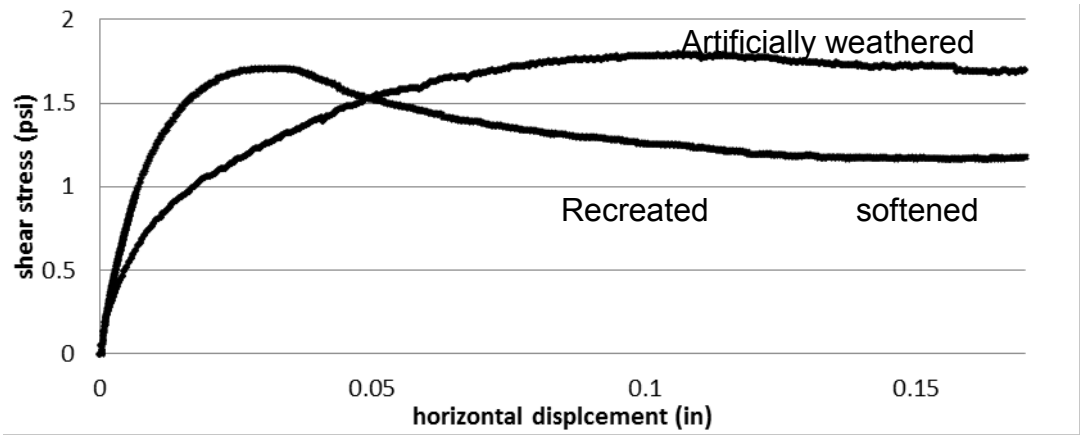

Figure_APX_A 16. Typical shear curve for cyclic sample and sample recreating softened conditions under 2psi confining pressure (from Bourasset 2013)

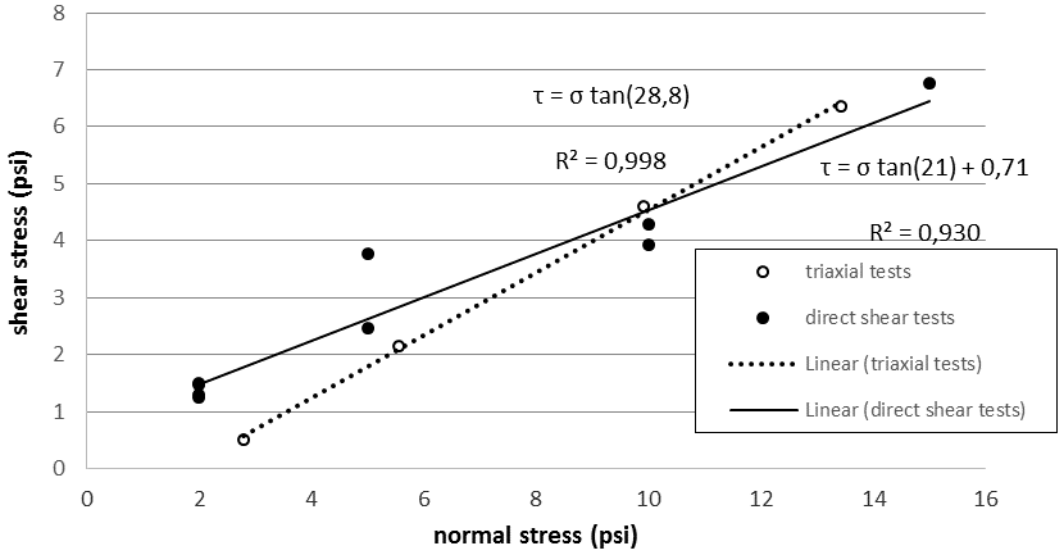

Figure_APX_A 17. Comparison of peak strength from direct shear and triaxial tests (from Bourasset 2013)

From the graph in A17, it can be noticed that the failure envelope corresponding to the direct shear tests exhibit a lower friction angle and a higher cohesion than the failure envelope from triaxial test. It results in higher shear strength values for lower normal stress. This difference is probably due to the mode of failure.

Table_APX_A 3. Inclinometer 2 Logs (From the ODOT Materials Division)

AASHTO Class	Description	Depth (feet)			L.L.	P.I.	Percent Passing			
							#4	#10	#40	#200
A-7-6(23)	Sandy Fat Clay	0.0	-	1.0	62	40	92	78	71	62.5
A-7-6(5)	Clayey Sand	1.0	-	2.0	54	32	85	55	42	35.7
A-7-5(20)	Sandy Fat Clay	2.0	-	3.0	76	44	89	67	57	53.7
A-1-b(0)	Poorly Graded Sand with Silt	3.0	-	4.0	NP	NP	89	58	16	9.7
A-7-6(11)	Clayey Sand	4.0	-	5.0	46	31	93	83	60	49.8
A-7-6(48)	Fat Clay with Sand	5.0	-	6.0	77	54	97	90	86	83.1
A-7-6(61)	Fat Clay	6.0	-	7.0	79	54	100	100	99	98.1
A-7-6(62)	Fat Clay	7.0	-	8.0	78	54	99	99	99	98.7
A-7-6(56)	Fat Clay	8.0	-	9.0	74	51	100	99	98	96.7
A-7-6(16)	Clayey Sand	9.0	-	10.0	66	45	93	67	51	48.3
A-7-6(49)	Fat Clay	10.0	-	11.0	68	47	99	96	95	94.5
A-7-6(56)	Fat Clay	11.0	-	12.0	73	49	100	99	99	98.7
A-7-6(58)	Fat Clay	12.0	-	13.0	76	50	100	100	100	99.4
A-7-6(38)	Fat Clay with Sand	13.0	-	14.0	76	52	93	80	74	72.2
A-7-6(52)	Fat Clay	14.0	-	15.0	70	46	100	99	99	98.1
A-7-6(54)	Fat Clay	15.0	-	16.0	71	47	100	100	100	99.3
A-7-6(54)	Fat Clay	16.0	-	17.0	71	48	100	99	99	98.3
A-7-6(54)	Fat Clay	17.0	-	18.0	68	49	100	100	100	98.8
A-7-6(5)	Clayey Sand	18.0	-	19.0	42	25	92	72	51	40.0
A-2-6(0)	Limestone (Clayey Sand with Gravel)	19.0	-	20.0	37	22	75	41	24	16.7
	Dry at end of drilling, and 24-hrs.									

Table_APX_A 4. Inclinometer 1 Logs (From the ODOT Materials Division).

SPT "N" (blows/ft)	AASHTO Class	Description	Depth (feet)			L.L.	P.I.	Percent Passing			
								#4	#10	#40	#200
15	A-7-5(48)	Fat Clay	0.0	-	0.5	75	42	100	100	98	93.9
		Clayey Sand with Gravel	0.5	-	1.0			75	58	46	41.0
	A-2-6(0)	Poorly Graded Sand with Clay and Gravel	1.0	-	1.5	40	24	60	30	14	11.5
49R(3.5")			1.5	-	2.0			95	64	54	50.2
	A-7-6(14)	Clayey Sand	2.0	-	2.5	64	43	90	71	53	46.9
	A-2-7(1)	Clayey Sand with Gravel	2.5	-	3.0	51	32	64	35	21	17.5
7	A-7-6(23)	Gravelly Fat Clay with Sand	3.0	-	3.5	67	48	72	68	60	56.5
	A-7-6(42)	Fat Clay with Sand	3.5	-	3.9	70	49	100	94	84	80.7
	A-7-6(45)	Fat Clay with Sand	3.9	-	4.5	76	55	95	87	81	78.7
6	A-7-6(70)	Fat Clay	4.5	-	5.0	88	60	100	100	99	99.0
	A-7-6(66)	Fat Clay	5.0	-	5.5	83	56	100	100	100	99.6
	A-7-6(71)	Fat Clay	5.5	-	6.0	87	62	100	100	99	98.6
11		Fat Clay	6.0	-	6.5	69	47	100	100	99	99.0
	A-7-6(37)	Fat Clay	6.5	-	7.0	60	39	100	100	95	87.9
	A-7-6(54)	Fat Clay	7.0	-	7.5	71	46	100	100	100	99.8
26		Fat Clay	7.5	-	8.0			100	100	99	97.8
	A-7-6(62)	Fat Clay	8.0	-	8.5	79	55	100	100	99	97.7
	A-7-6(35)	Fat Clay with Sand	8.5	-	9.0	72	50	87	83	74	70.1
16	A-7-6(57)	Fat Clay	9.0	-	9.5	74	49	100	100	100	99.8
	A-7-6(58)	Fat Clay	9.5	-	10.0	74	50	100	100	100	99.6
		Missing	10.0	-	10.5						
28R(1.75")	A-7-6(59)	Fat Clay	10.5	-	11.0	78	51	100	100	100	99.4
	A-7-6(53)	Fat Clay	11.0	-	11.5	73	46	100	100	100	99.6

Table A5 (Continued). Inclinometer 1 Logs (From the ODOT Materials Division).

SPT "N" (blows/ft)	AASHTO Class	Description	Depth (feet)			L.L.	P.I.	Percent Passing			
								#4	#10	#40	#200
	A-7-6(24)	Sandy Fat Clay	11.5	-	12.0	65	44	96	83	64	60.7
21	A-7-6(53)	Fat Clay	12.0	-	12.5	71	46	100	100	100	99.4
	A-7-6(53)	Fat Clay	12.5	-	13.0	70	46	100	100	100	99.2
	A-7-6(53)	Fat Clay	13.0	-	13.5	71	46	100	100	100	99.4
19	A-7-6(52)	Fat Clay	13.5	-	14.0	72	44	100	100	100	99.6
	A-7-6(48)	Fat Clay	14.0	-	14.5	66	42	100	100	100	99.6
	A-7-6(54)	Fat Clay	14.5	-	15.0	71	46	100	100	100	99.6
22	A-7-6(48)	Fat Clay	15.0	-	15.5	68	43	100	100	98	96.4
	A-7-6(47)	Fat Clay	15.5	-	16.0	65	43	100	100	98	97.1
	A-7-6(47)	Fat Clay	16.0	-	16.5	65	42	100	100	99	97.9
50R(2.5")	A-7-6(46)	Fat Clay	16.5	-	17.0	68	44	95	95	94	93.4
	A-7-6(13)	Sandy Lean Clay	17.0	-	17.4	46	26	100	97	74	60.8
	A-2-6(0)	Clayey Sand with Gravel	17.4	-	18.0	33	18	82	52	27	19.9
	A-2-6(0)	Limestone (Clayey Sand with Gravel)	18.0	-	19.0	30	16	81	53	31	21.7
	A-1-a(0)	Limestone (Well-Graded Sand with Silt and Gravel)	19.0	-	20.0	NP	NP	58	27	11	6.8
		Dry at end of drilling									
		Inclinometer casing installed within 4-hrs of end of drilling.									

Appendix B – Locations and Details of ODOT Identified Landslides

Division 3 Landslides: April 25th, 2012 Landslide Fieldtrip

The landslides to be visited included the following locations. The total travel distance about 240 miles roundtrip. The team left at 8:15 am and returned at 6:30 pm.

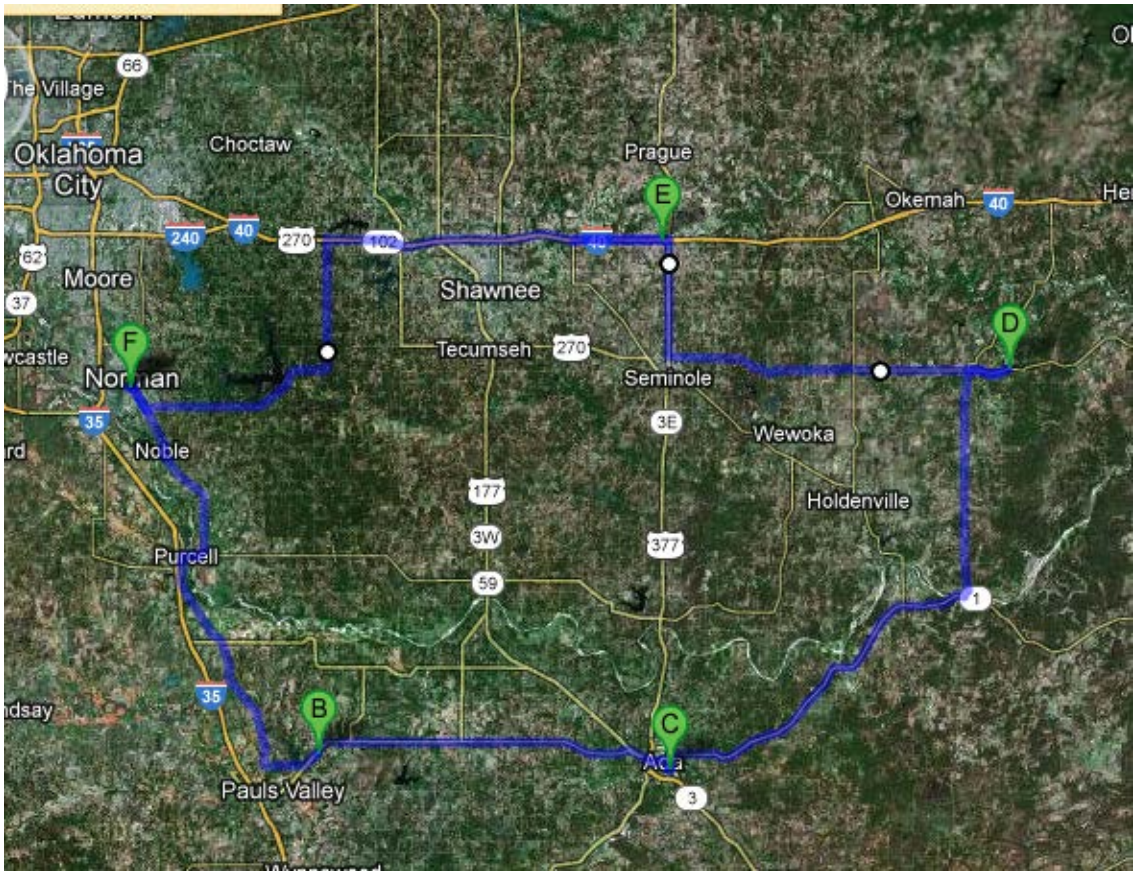

Figure_APX_B 1. Map of Division 3 Landslide Locations.

Table_APX_B 1. NRCS USDA Soil Survey Soil Information for Division 3 Slide Locations.

Site Name	Soil Type	Classification		Liquid Limit (%)	Plasticity Index (%)	Comment
		USGS	AASHTO			
HW19 (possible)	Grainola clay loam	CH, CL, SC	A-6, A-7	33-60	12-34	There is bedrock below 2.92 ft.
	Renfrow silt loam	CH, CL	A-4, A-6, A-7	30-60	15-34	No bedrock from 0 to 5.25 ft.
HW3 near Ada	Heiden clay	CH, CL	A-7-6	51-80	32-55	No bedrock from 0 to 6 ft.
	Durant loam	CH, CL	A-4, A-6, A-7	30-70	21-39	No bedrock from 0 to 5.83 ft.
Route 9 Wetumka	Hector-Endsaw complex	GC-GM, GM, SC-SM, SM, CH, CL	A-2, A-4, A-7	0-25 41-60	NP-7 18-32	Depth of bedrock varies from 0.9 to 4 ft.
I40 and HW99 Junction	Chickasha loam	CL-ML, ML, CL, SC	A-4, A-6	25-40	7-18	There is bedrock below 4.67 ft.

Stop 1: Route 19, Intersection with Hines Road (ECR 1540), on left side (across from Hines)

Figure_APX_B 2. Route 19, Intersection with Hines Road (ECR 1540).

Lat: 34°46’ 57” N,
Long: 97°10’ 31” W

Height of Slope: 17.25’
Width of slide block: ~150’ (estimated, since this slide is fixed already, and not moving anymore)
Landcover: knee high grass
Desiccation crack: None noticeable
Rainfall before the trip date: 3.43”, Mesonet Location = Pauls Valley, April 1-25, 2012
Type of slip surface: Slide fixed

Visual Classification of Soil:

Table_APX_B 2: Route 19 (N/W side) intersection with Hines

Depth (ft)	% water content	Visual Classification
0.5		Top soil, gravel from road
1	18.98	
1.5		Dark red/brown fat clay with <5% silt
2	16.63	
2.5		Dark red/brown silty sand with little clay
3	17.39	Dark brown fat clay with silt
3.5		
4	18.32	Mottled red/brown to orange red fat clay with little silt

Slide notes: This slide was fixed 15 years ago. No current problems noted. Mike Wilson (405-248-7962) met us on site to give us a history of the slide. Somewhere in the vicinity of 1997-98 the slide was repaired. ODOT started having problems with it after the toe got disturbed by digging a pipeline. The slide was 6-8' out into the driving surface, and they performed constant maintenance by overlaying the pavement. The soil was always wet. Water was the main issue. They don't remember putting in any drainage measures. Installed a sheet pile wall about 15-20' deep, about 15' off the road, for about 80 feet parallel to the road. This length was estimated based on the change in vegetation along the sheet pile and at the edges. There was an obvious shift in height and color of vegetation at both sides. It is unlikely that fill was brought in. Hand auger pulled up relatively fat clay.

Stop 2: Gabion retaining wall fix on Route 377, south of Ada.

Notes: Only latitude and longitude plus pictures were recorded for this slide, as it was fixed already.

Lat: 34°45'55.74"N
Long: 96°40'13.26"W

Figure_APX_B 3. Ariel shot of problematic Area after fix (note Gabion Walls on left side of road).

Figure_APX_B 4. Gabion Wall as Retaining Structure.

Figure_APX_B 5. Gabion Wall as Retaining Structure.

Stop 3: Route 9, 3.5 miles east of Wetumka

Lat: 35°14'2.93"N
Long: 96°11'2.30"W

Height of Slope: 20’
Width of slide block: ~370’
Landcover: Tall deciduous trees, with some small cedars, brambles
Desiccation crack: None noticeable
Rainfall before the trip date: 1.85”, Mesonet Location = Holdenville, April 1-25, 2012
Type of slip surface: Probably circular, but 4, 3’ layers of Gabion Baskets, 240’ long, were added to the toe, so it is hard to tell. The road has continuous maintenance with asphalt overlays.

Visual Classification of Soil: Fat clay overlaying relatively sandy soil, but the slope is very steep.

Table_APX_B 3. Water Content and Visual Classification of Boring Hole in Slide Mass on Route 9, 3.5 miles east of Wetumka (see location in Figure B6).

Depth (ft)	% water content	Visual Classification
0.5	11.09	Top soil
1		
1.5	10.38	Brown sand w/ trace clay w/ occasional rocks/nodules
2		
2.5	15.79	Sand w/ trace clay, brown/tan
3		Change occurred to greenish/white/tan fat clay
3.5	14.72	Tannish brown mottled clay, then turning to sand. Nail can scrape clay off "rock" chunks
4		

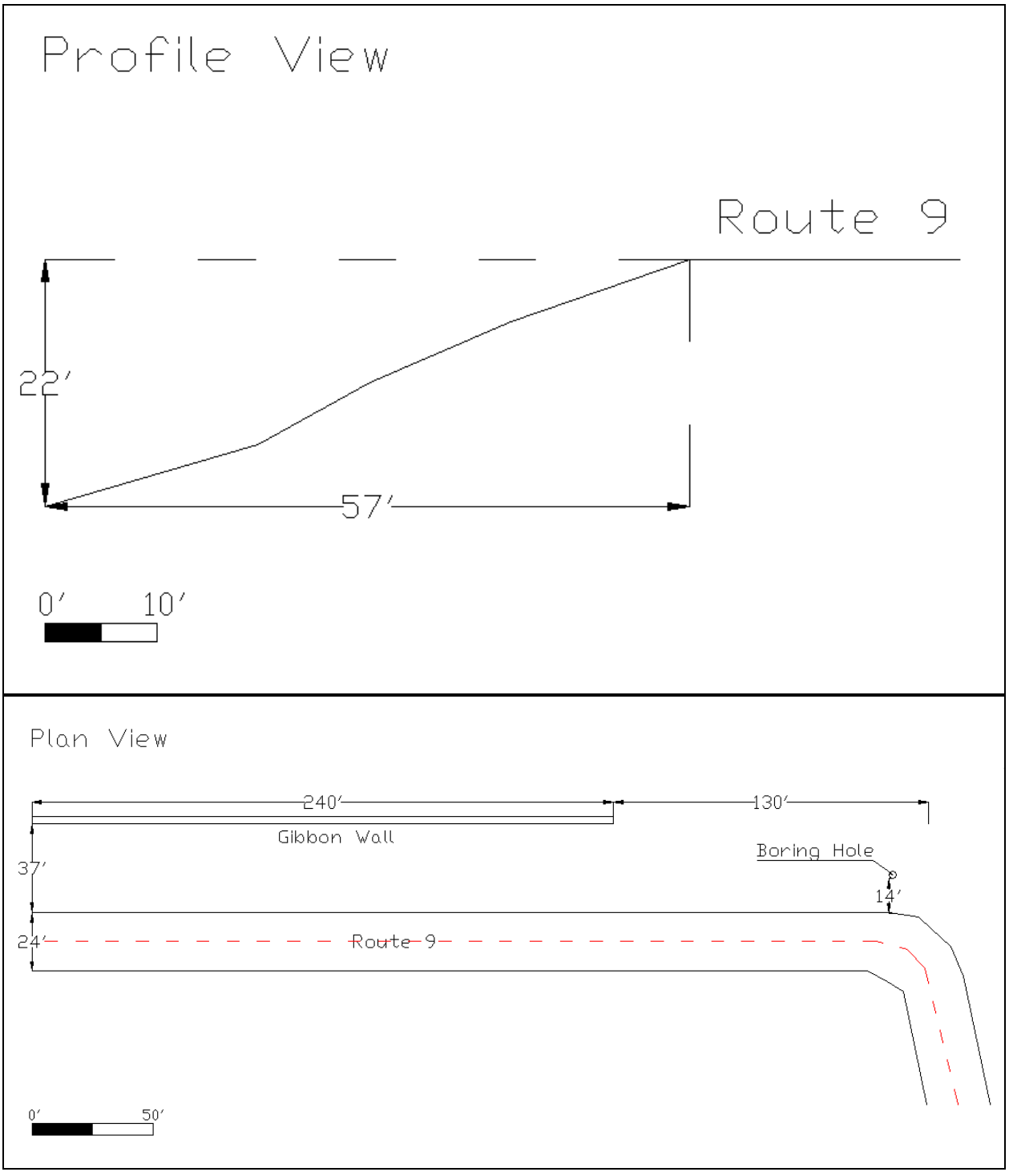

Figure_APX_B 6. Route-9 – Wetumka Landslide

Notes: Very steep slope, on a curve in road. Asphalt overlays approaching bottom of guardrail, and at the ends of the 240' long gabion basket retaining wall, the road is noticeably moving faster than the center part of the slide. The road was realigned by a few feet several years back to move the road away from the slope, however, slope is still slowly moving. See field sheet for sketch of slide.

Figure_APX_B 7. Looking west on Route 9. Landslide on the north side of road.

Figure_APX_B 8. Can see old guardrail almost buried down the slope. The road was slightly realigned away from the slope a few years ago, although it is still moving.

Figure_APX_B 9. Old Guardrail is seen here actually acting as a retaining measure for additional asphalt overlays.

Figure_APX_B 10. 240’ long row of Gabion Baskets, stacked 4 high in stair step fashion.

Stop 4: Eastbound I-40, about 1 mile before Seminole (200) Exit on Backslope

Lat: 35°23'2.04"N
Long: 96°41'0.56"W

Height of Slope: 12.5'
Width of slide block: ~90'
Landcover: Knee high grass, weeds
Desiccation crack: yes, surface very dry
Depth of water Table: 3.5-4.0' below middle of slope, found in hand auger hole.
Rainfall before the trip date: 2.52", Mesonet Location = Shawnee, April 1-25, 2012
Type of slip surface: Probably circular, or shallow block.

Visual Classification of Soil: Grey clay starting to have moisture around 2-3', turning to stiff grey clay, and water table at 4'.

Table_APX_B 4: East I-40, 1 mile before Seminole exit (casino) (BH3)

Depth (ft)	% water content	Visual Classification
0.5	16.71	Dry, grey, crumbly clay slope riddled with cracking
1		
1.5	19.69	Dry, grey, crumbly clay
2		
2.5	19.65	Grey clay, starting to have moisture
3		
3.5	27.99	Grey stiff clay, hit very wet soil at 3.5'
4		
4.5	23.82	Wet, stiff grey clay

Notes: Slide is approximately 150 feet east of the Exit 200 sign, and the toe is about 23' from the edge of the eastbound shoulder. There is no chance of the slide affecting the roadway, although it certainly affects maintenance. The slide is about 60 feet in length and 90 feet wide at the largest dimensions. The slope is not steep. A high water table in extremely fat clay seems to be the problem. Drove past this again on May 9th, and it looks to have been mowed, so maintenance crews are not having a problem getting on and around the slide.

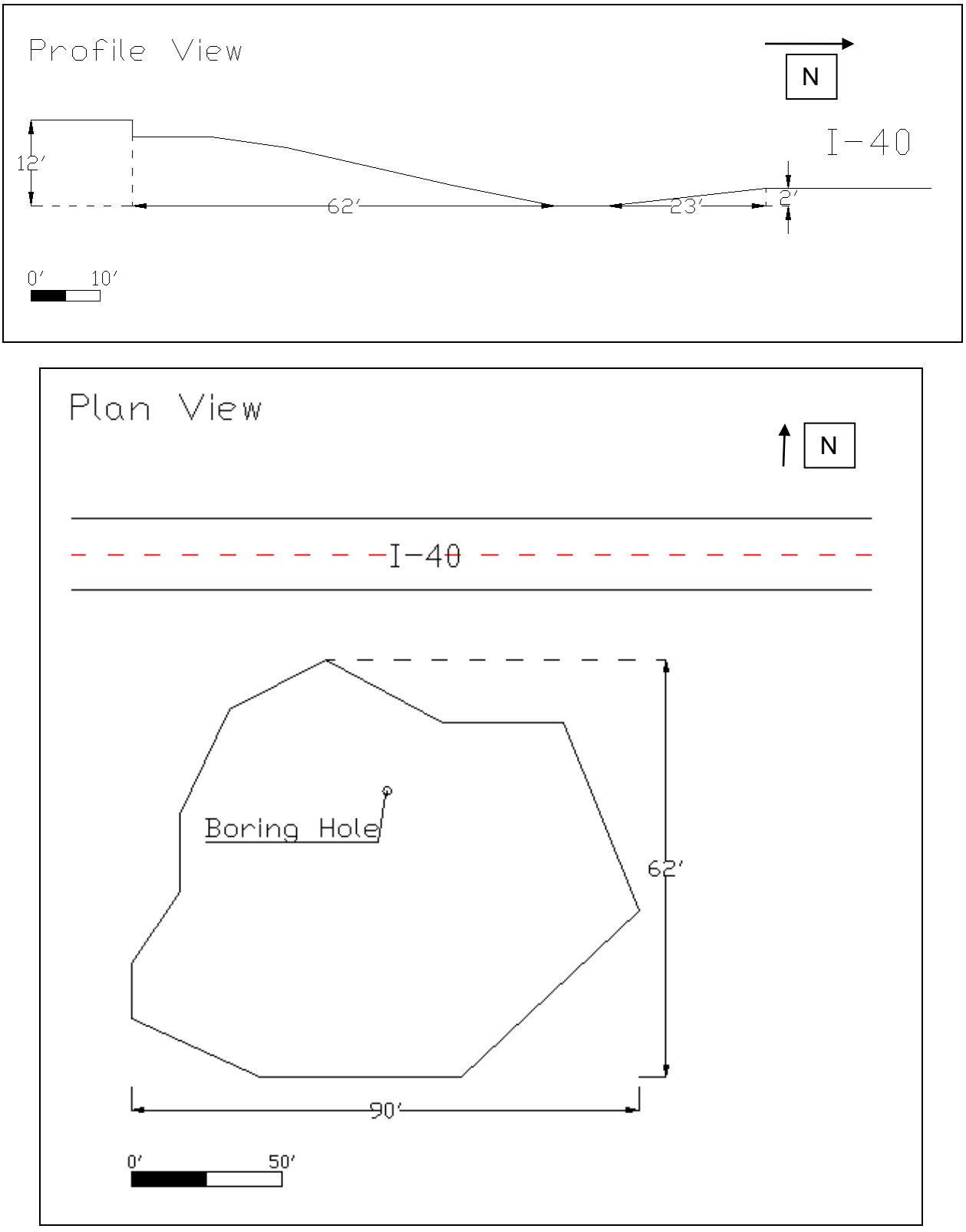

Figure_APX_B 11. I-40 – Seminole Landslide

Figure_APX_B 12. Satellite photo of slide outline. Note location of Exit sign in center left of photo, below eastbound I-40.

Figure_APX_B 13. Desiccation Cracks all over slope, although water was found only 4 feet below the surface.

Figure_APX_B 14. Looking back at the slide mass.

Figure_APX_B 15. Can see the headscarp here as a change in vegetation cover.

Division 2 Landslides: May 9th, 2012 Landslide Field trip

The landslides to be visited included the following locations. The total travel distance was 477 miles. The team left at 7:45 am and returned at 8:30 pm.

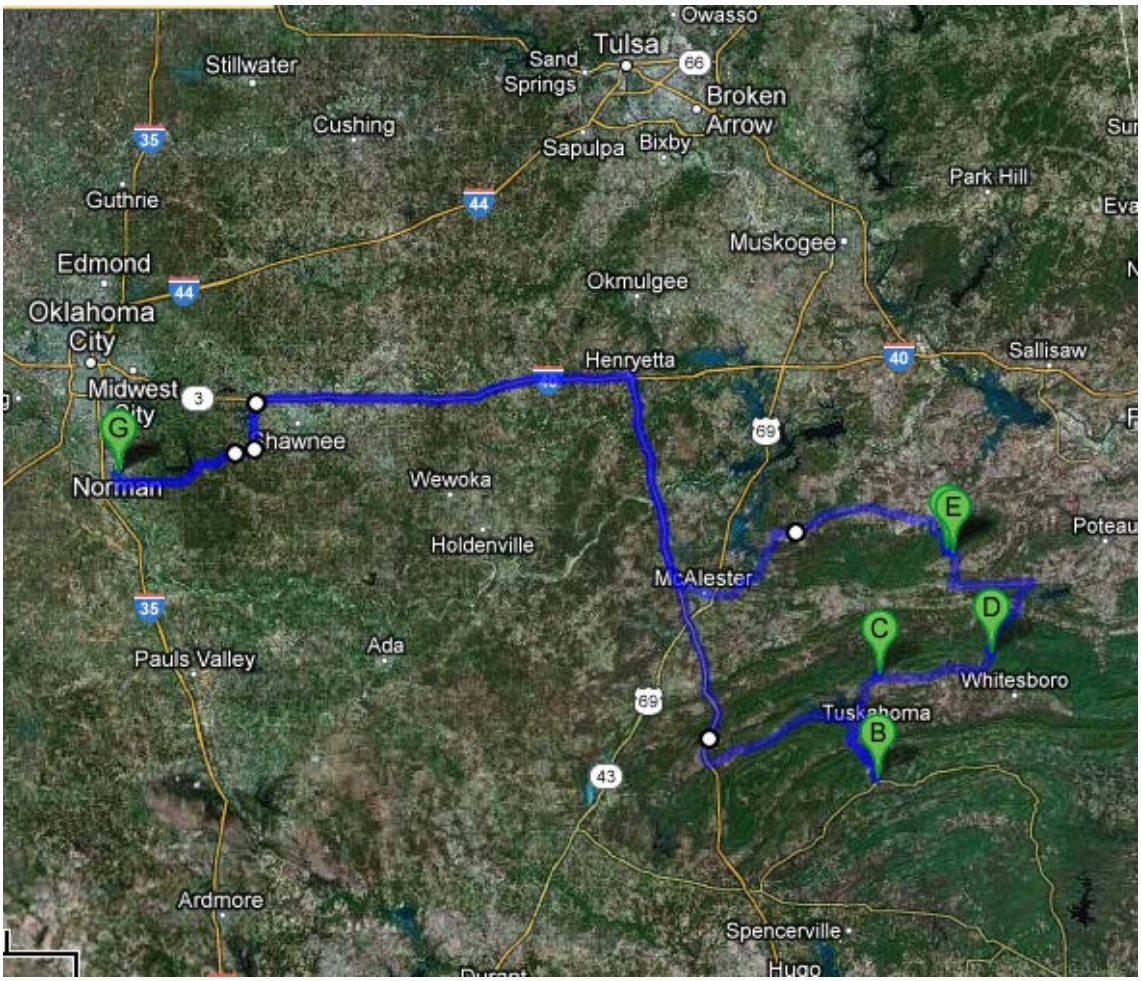

Figure_APX_B 16. Division 2 Landslide Locations.

Table_APX_B 5. NRCS USDA Soil Survey Soil Information for Division 2 Slide Locations.

Site Name	Soil Type	Classification		Liquid Limit (%)	Plasticity Index (%)	Comment
		USGS	AASHTO			
US 271 and US 144 junction	Carnasaw-Pirum-Clebit association	SM, SC, SC-SM, CH, CL, GC-GM, GM, GC	A-2, A-4, A-6, A-1, A-7	0-30 37-65 15-30	NP-10 18-35 3-10	Depth of bedrock varies from 1 to 3.42 ft.
US 271, Talihina	Pirum-Octavia-Panama association	SC-SM, CL, CL-ML, SM, ML, SC-SM, GC-GM, GM,	A-6, A-1, A-2, A-4, A-7	14-20 25-40 37-60	NP-3 8-18 16-34	There is bedrock below 2.5ft.
US 271, Talihina (possible)	Pirum-Octavia-Panama association	SC, SC-SM, CL, CL-ML, GC-GM, GM, SC-SM, SM	A-6, A-1, A-2, A-4, A-7	14-26 25-40	NP-7 8-18	There is bedrock below 2.5ft.
Rt. 82, Red Oak Slide No.1	Carnasaw-Clebit association	CL-ML, SC-SM, CH, CL GC-GM,	A-1, A-2, A-4, A-6, A-7	0-30 41-65 30-37	NP-10 18-35 8-14	Depth of bedrock varies from 1 to 3.83 ft.
Rt. 82, Red Oak Slide, No.2	Carnasaw-Clebit association	SM, CL-ML, SC, CL,CH, GC-GM	A-1, A-2, A-4, A-6, A-7	0-30 31-37 41-65	NP-10 8-14 18-35	Depth of bedrock varies from 1 to 3.83 ft.
	Carnasaw-Pirum-Clebit association	CH, CL, SC-SM, CL-ML, SC, GM	A-1,A-2,A-4, A-6, A-7	15-30 30-65 0-26	3-10 8-35 NP-7	Depth of bedrock varies from 1.3 to 4.2 ft.
	Ceda-Rubble land complex	GC-GM, GM, SC-SM, SM, GP	A-1,A-2,A-4, A-6	15-40	NP-18	No bedrock from 0 to 6 ft.
Route 70, Idabel	Cadeville loam	ML, CH, CL	A-4, A-6, A-7	20-38 40-60	2-19 22-35	Below 6 ft, there is bedrock.
	Swink-Hollywood complex	CH, CL	A-6, A-7	37-60 25-45 51-75	19-39 11-25 25-45	

Stop 1: Pushmahata County, Route 271, 2 miles north of junction 144

Lat: 34.4974
Long: 95.2799

Height of Slope: 17.25'
Width of slide block: 138'
Landcover: Pine trees at base of embankment, small mimosa type trees on slope, with knee high grass
Desiccation crack: None noticeable
Rainfall before the trip date: Surface soil very wet: 3.5", Mesonet Location = Clayton, April 9-May 9, 2012
Type of slip surface: circular

Visual Classification of Soil: Surface soil is red, fat clay with silt, but the deeper you get, the soil is less clayey with numerous limestone/sandstone chunks. Very difficult to hand auger. Took a water content from center of slide at 1 foot depth.

Table_APX_B 6. Route 271, Pushmahata County, 2 miles north of jct 144

Depth (ft)	% water content	Visual Classification
1	13.97	Surface soil is fat clay w/ silt. Deeper soil less clayey w/ limestone/sandstone chunks. Difficult to hand-auger

Slide notes: Slide is active and maintained monthly. Maintenance includes adding chipseal and asphalt to level the road surface. Took a water content from the center of slide at 1 foot depth.

B18. A. Cracking in the road bed.

B. Example of subsurface encountered.

C. Depth of Asphalt overlay

D. Vegetation.

Figure_APX_B 17. Cracking in the road bed (A). Example of subsurface encountered (B). Depth of Asphalt overlay (C). Vegetation (D).

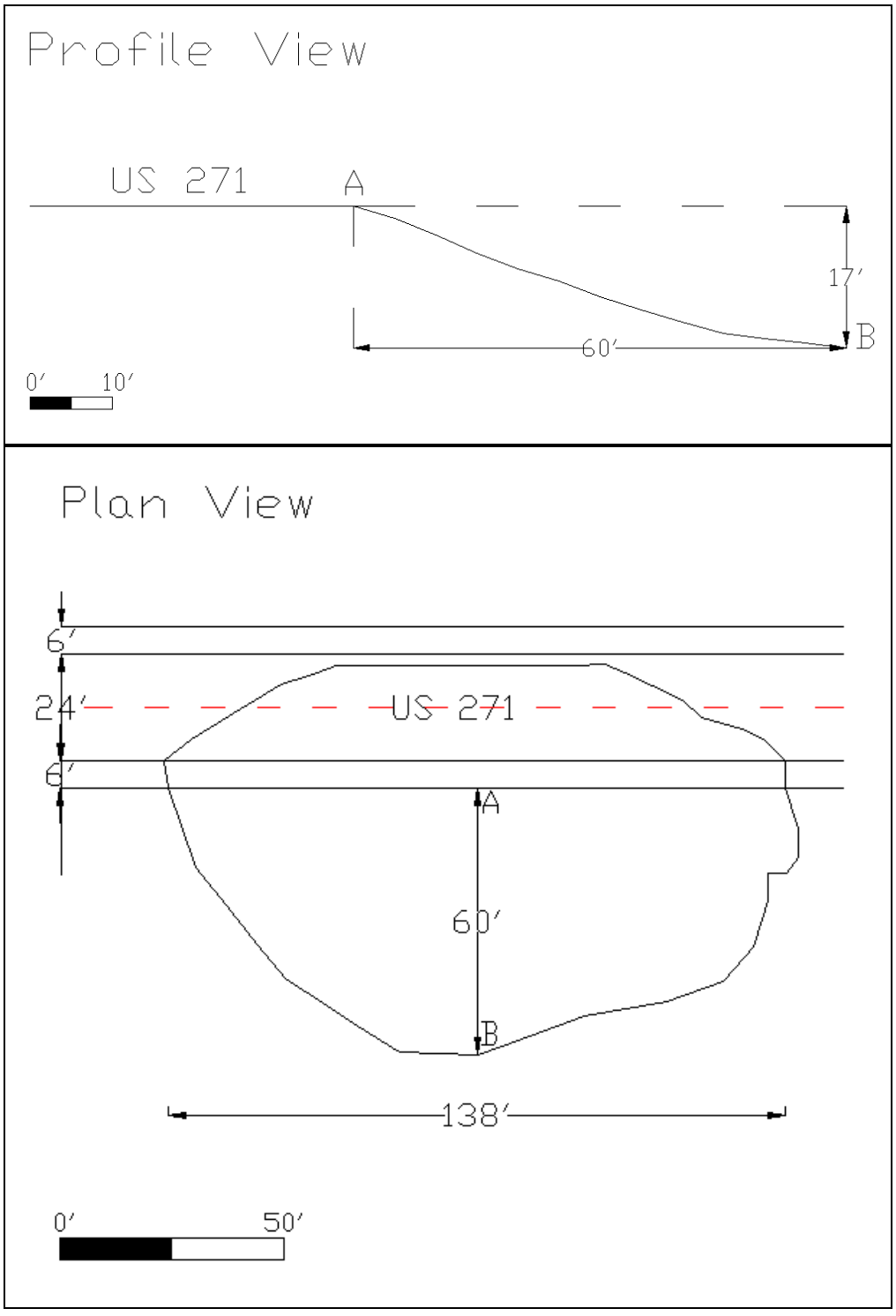

Figure_APX_B 18. US-271 – Clayton Landslide

Stop 2: Route 1/2/63, 1 mile north of 271 junction, past village station, over hill, round curve, on right, no guard rail

Figure_APX_B 19. Shoulder pavement overlays.

Lat: 34°44’30”N
Long: 95°16’32”W

Height of Slope: ?
Width of slide block: ?
Landcover: Pine trees
Desiccation crack: None noticeable
Rainfall before the trip date: 3.5”, Mesonet Location = Clayton, April 9-May 9, 2012

Type of slip surface: ?

Visual Classification of Soil: No hand auger was done because we could not positively identify the location of the slide.

Slide notes: Project team had difficulty finding this location. Asphalt overlays only in northbound shoulder and no cracking could be seen in the roadbed. The project team could not locate the toe of the slide, nor could ODOT Division Maintenance engineers. ODOT Division 2 maintenance records show significant continuous asphalt overlays on the northbound shoulder, however. This may be due to settlement, dispersive soils or slow creep, although the trees on the steep slope are not tilted. Creek bed runs parallel with road at this point. Project team did not soil sample.

Stop 3: Route 271, after Talimena state park, and between an abandoned tavern on right and Talihina Drive (State Highway 88). Slide is on south-west side of 271 in the middle of an S-curve.

Lat: 34.7934
Long: 94.9539

Height of Slope: very steep and covered in dense vegetation – High - Could not survey slide.
Width of slide block: 210 feet at road surface
Landcover: Pine trees, cedar, beech, elms lower on the slope and grasses high on slope. There were some visible tree stumps close to roadway, so original slope must have been heavily tree covered.
Desiccation crack: None noticeable
Rainfall before the trip date: 3.06", Mesonet Location = Talihina, April 9-May 9, 2012.

Depth of water table: 65" below standpipe riser top, which was located about 5 feet away from guard rail. Water monitoring well installed by ODOT.
Type of slip surface: Most likely circular

Visual Classification of Soil: Slope was too steep to hand auger, however, the pickax was used to scrape the surface and dig about 1.5' into the slope, and very wet, light brown fat clay with weak shale pieces interbedded was discovered. There were also larger chunks of limestone and mudstone.

Table_APX_B 7. Route 271, Talihina

Depth (ft)	% water content	Visual Classification
1	21.67	Limestone/mudstone, very wet, fat clay, light brown, w/ shale pieces interbedded

Slide notes: This is an active slide, where the current remediation is asphalt overlays to bring the road to the correct elevation. From what the project team could see, there was approximately 36" of asphalt visible above the existing ground line.

Figure_APX_B 20. Route 271, after Talimena state park Looking south.

Figure_APX_B 21. Route 271, after Talimena state park Looking north. Project team is measuring water table depth in monitoring well.

Figure_APX_B 22. Route 271, after Talimena state park Looking north. 3 feet of asphalt overlay visible.

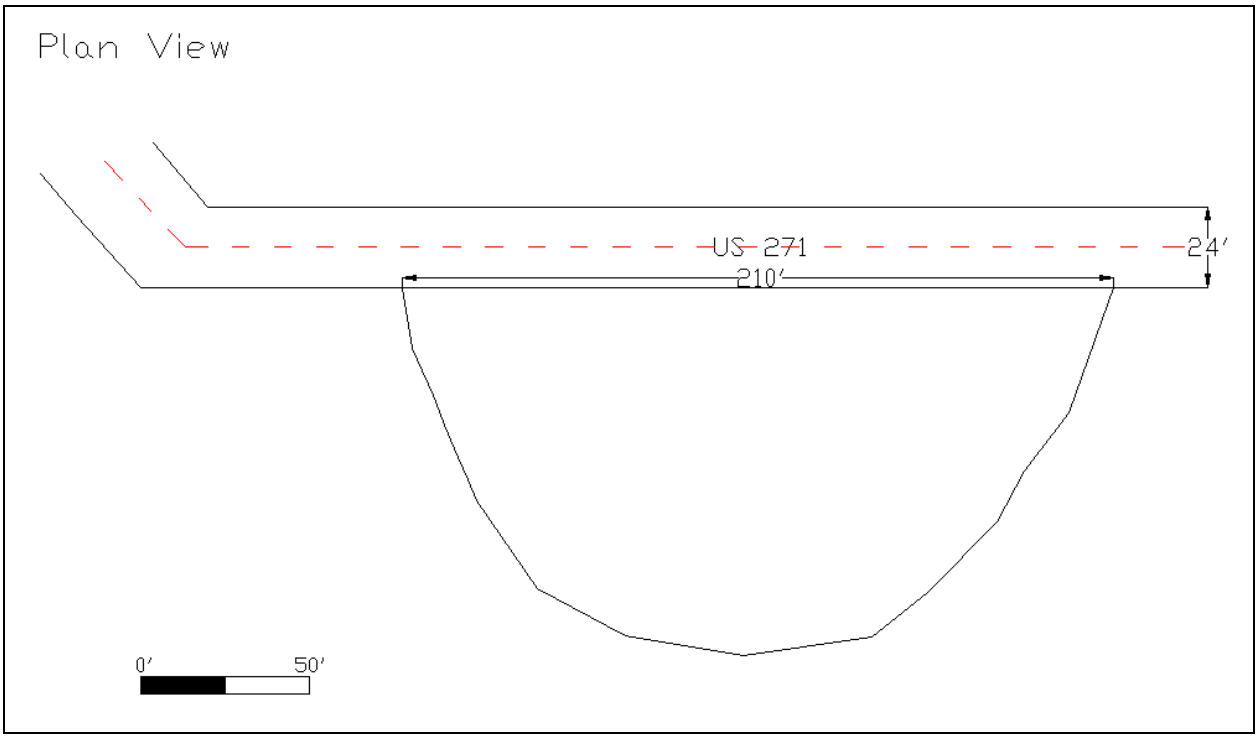

Figure_APX_B 23. US-271 – Talihina Landslide

Stop 4: Route 82 Landslide north of Red Oak, on west side of highway.

Lat: 35.02422
Long: 95.0627

Height of Slope: This landslide is currently being fixed.
Width of slide block: Very large
Landcover: nothing at the moment.
Desiccation crack: None noticeable
Rainfall before the trip date: 3.75", Mesonet Location = Wilburton, April 9-May 9, 2012.

Depth of water table:
Type of slip surface: Shallow block failure over wet shale deposit.

Visual Classification of Soil:

Slide notes: This was a big slide that occurred in late 2007/early 2008. Currently, this slide is being remediated and is under construction. For photos of the slide as it looked before construction, please see http://learys.smugmug.com/Work/Engineering-Geology-Landslides/4396561_wXCqK5#!i=258205353&k=oC4q5.

Figure_APX_B 24. Repairing the slide.

Stop 5: Route 82 Landslide north of Red Oak, on west side of highway.

Lat: 35°2'10.05"N
Long: 95°4'53.60"W

Height of Slope: Very large. Too large to survey without total station.
Width of slide block: Very large
Landcover: Grasses
Desiccation crack: None noticeable
Rainfall before the trip date: 3.75", Mesonet Location = Wilburton, April 9-May 9, 2012.

Depth of water table:
Type of slip surface: Circular. Look at the headscarp.

Visual Classification of Soil:

Slide notes: This was a big slide that occurred prior to 2003 as determined from historical satellite photos. For photos of the slide as it looked in 2008, please see http://learys.smugmug.com/Work/Engineering-Geology-Landslides/4396561_wXCqK5#!i=258205353&k=oC4q5. There has been nothing done to this site since the slide occurred. This might be a good location to use as verification of the model.

Figure_APX_B 25. Photo taken May 9, 2012 standing at the end of destroyed county road.

Figure_APX_B 26. Current satellite photo of the landslide mass.

Idabel Landslide: A separate trip was made to this landslide and the geometry is shown below. All other lab and insitu data is shown in Appendix A, since this was the slide we decided to instrument for validation.

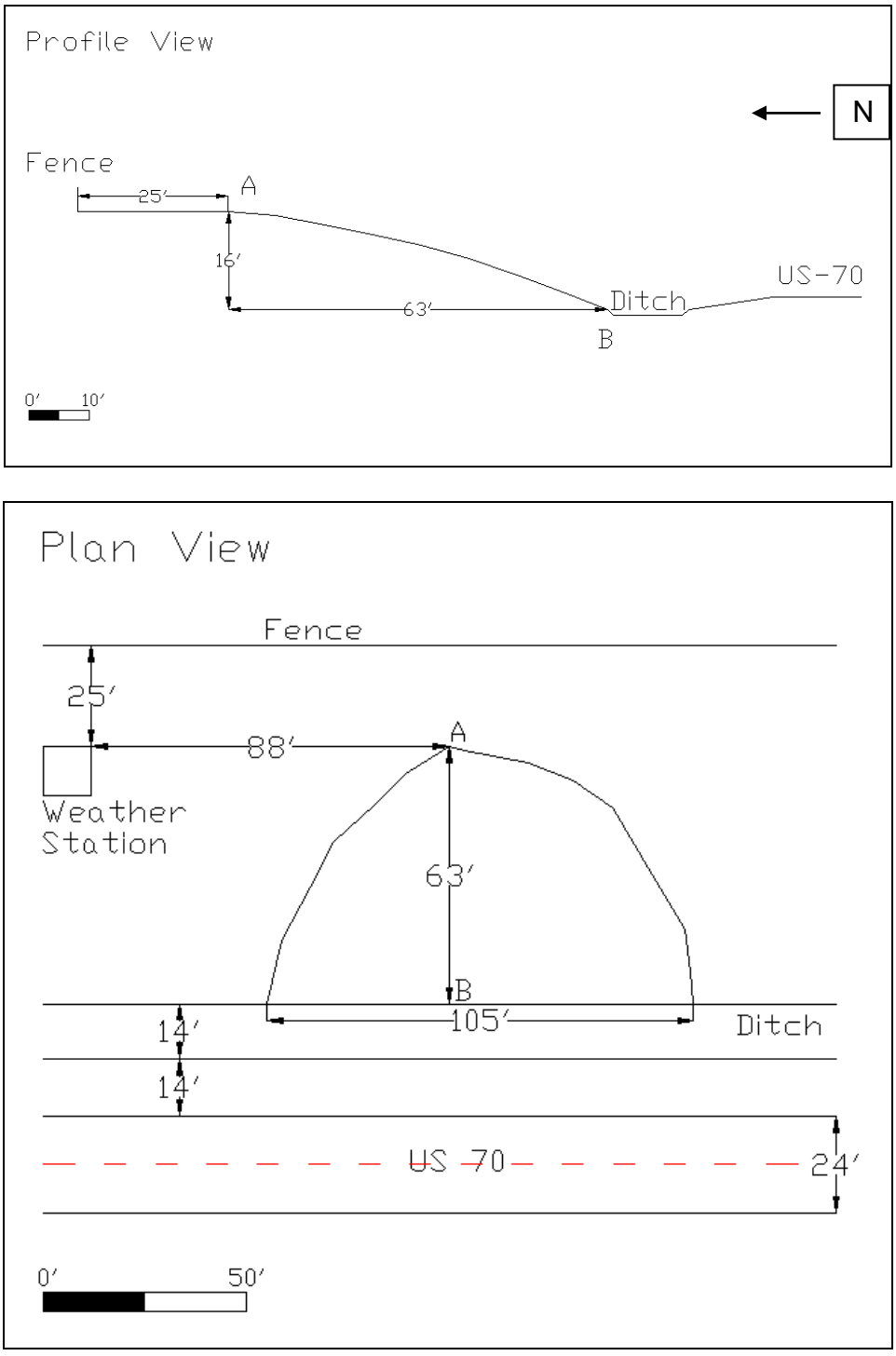

Figure_APX_B 27. Landslide in McCurtain County, just west of Idabel on the north side of US-70.

Division 1: May 24th, 2012 Landslide Field trip

Field Trip #3: A field trip was held to visit five sites in Division 1 on Thursday, May 24th, 2012. Of the five sites, all were active, however, two required more regular maintenance than the others. More details on each of the slides is given below. The landslides to be visited included the following locations. The total travel distance was 422 miles. The team left at 7:45 am and returned at 7:30 pm.

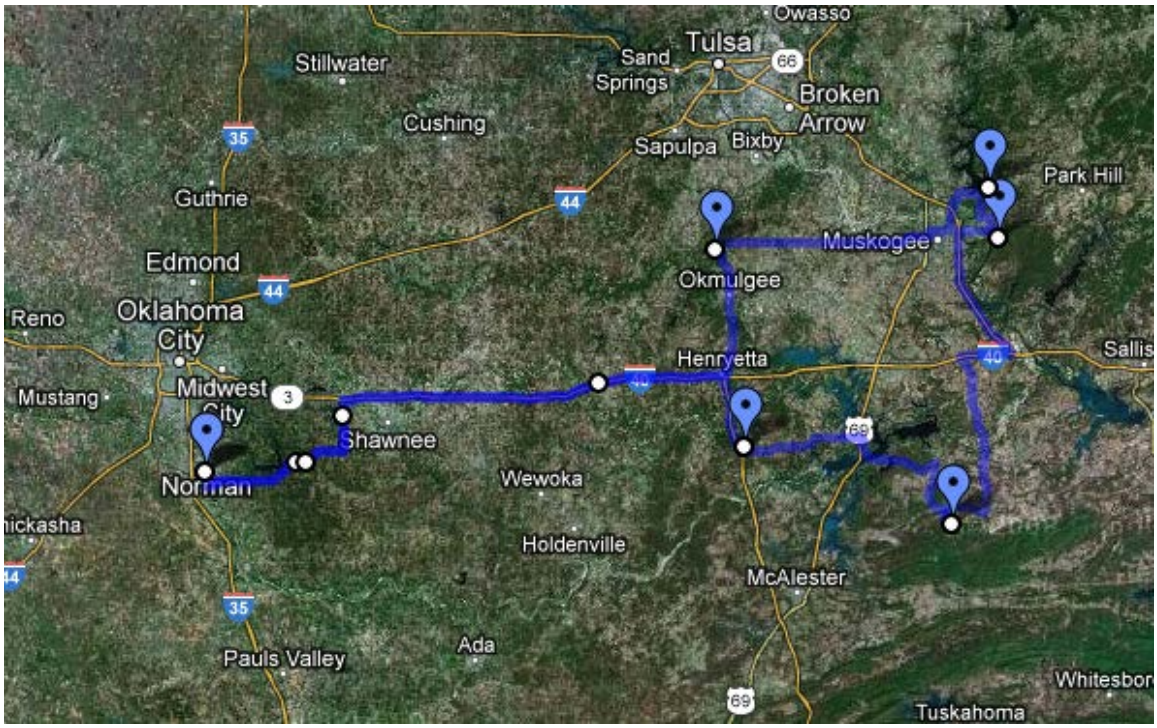

Figure_APX_B 28. Division 1 Field Trip Route and Landslide locations.

Table_APX_B 8: NRCS USDA Soil Survey Soil Information for Division 1 Slide Locations.

Site Name	Soil Type	Classification		Liquid Limit (%)	Plasticity Index (%)	Comment
		USGS	AASHTO			
Route 9 landslide	Talihina clay loam	CL, CH	A-7, A-6	37-50	15-26	Below 1.25 ft, there is bedrock
Hascal County, Highway 2 Landslide	Carnasaw-Bengal-Clebit complex	CH, CL, GC, GC-GM, GM	A-2, A-4, A-6, A-7	14-26 24-30 30-37 37-65	NP-7 4-10 8-14 18-35	Depth of bedrock varies from 1.25 to 3.5 ft.
Fort Gibson Dam Landslide	Britwater gravelly silt loam	SC, SC-SM, CL, CL-ML, , GC	A-2, A-4, A-6, A-7	0-38 30-50	6-15 11-23	There is no bedrock from 0 to 5.25 ft.
Highway 10 Landslide	Shidler-Rock outcrop complex	CH, CL	A-6, A-7	33-55	12-27	Rock outcrop
North bound lane 75 landslide	Hector-Endsaw complex	SC-SM, SM, GC-GM, GM, CH, CL	A-4, A-2, A-7	0-25 41-60	NP-7 18-32	Depth of bedrock varies from 1.25 to 3.5 ft.

Stop 1: Route 9, 1 mile east of Turnpike; several miles west of Eufala, on south side of road

Lat: 35°15'38"N
Long: 95°54'19"W

Height of Slope: 14.8'
Width of slide block: 234'
Landcover: high grass (full of chiggers) with tall deciduous trees at toe
Desiccation crack: Yes, small surface cracks
Rainfall before the trip date: 1.35", Mesonet Location = Eufala, May 1-24, 2012.
Type of slip surface: circular probably
Visual Classification of Soil: Very difficult to hand auger. Took a water content from center of slide every foot until refusal at 53". Soil was sandy at the top, and then reddish brown fat clay with silt. A change was seen at 40", where the soil became much more silty, but then returned to predominantly clay with chunks of limestone.

APX_B 9: Route 9, 1 mile east of turnpike, south side road

Depth (ft)	% water content	Visual Classification
1	15.67	Grey clay
2	14.56	
3	18.05	
3.5		Soil changed to silty
4	14.99	
4.4	15.09	Auger Refusal (hit rock)

Slide notes: Slide is active and maintained on a periodic basis. The last time this slide was maintained was 2010, where they put chip set and tar down to try to repair the roadway cracking. Maintenance includes adding chipseal and asphalt to level the road surface. Roadway was realigned sometime in the past by approximately 15 feet to the north for about 235'. The old white shoulder line is still visible. The Project team was unable to define the outline of the slide on slope due to dense vegetation and a not clear cracking pattern.

Figure_APX_B 29. Route 9, 1 mile east of Turnpike, road realignment and landslide cracking in new shoulder (old east bound lane) visible.

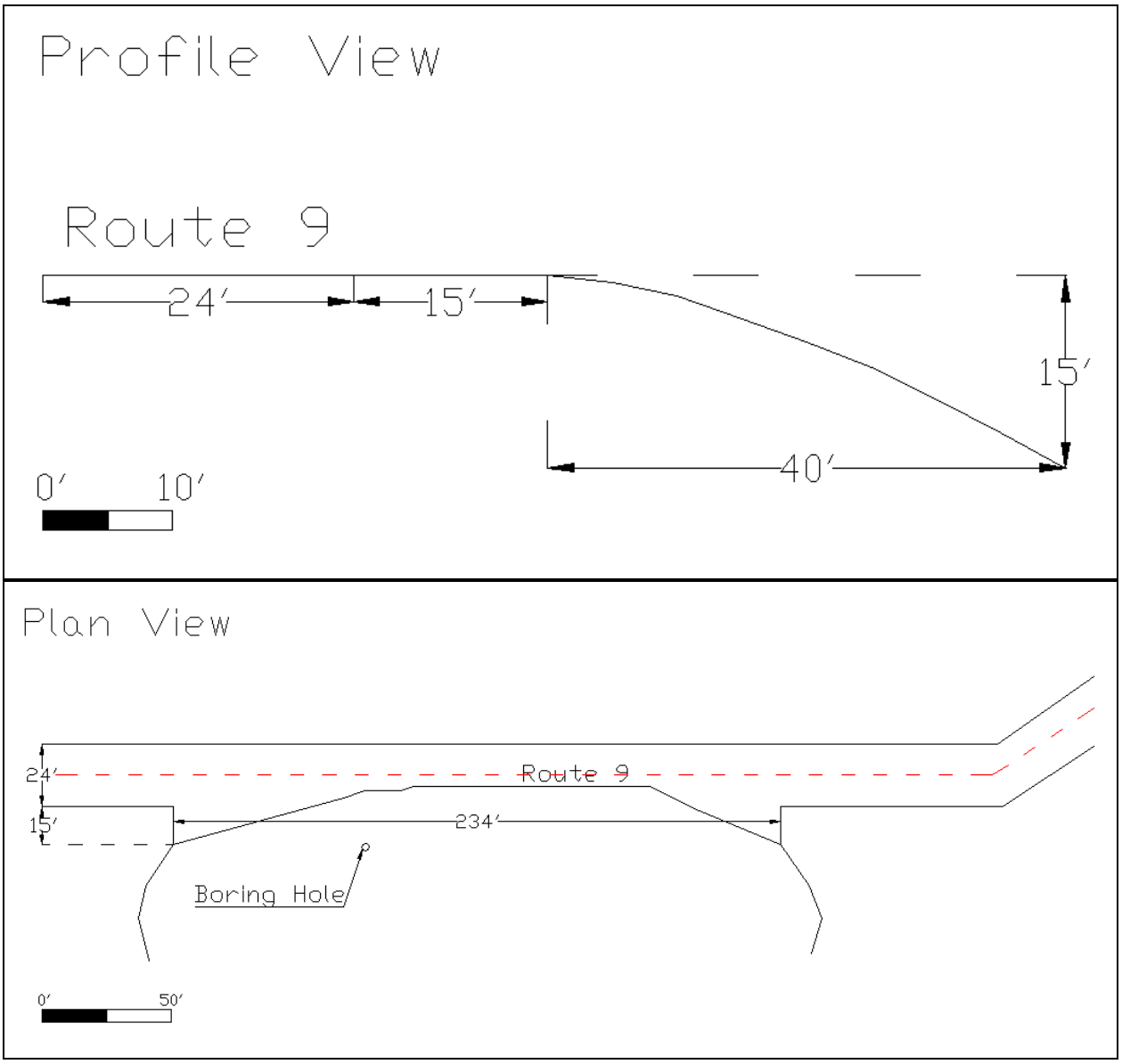

Figure_APX_B 30. Route 9 – Eufala Landslide

Stop 2: Route 2, 4 miles south of junction with Route 31; also north of Robber's Cave St. Park

Lat: 35°13'43"N
Long: 95°24'20"W

Height of Slope: unable to survey due to heavy overgrowth (trumpet vines, mimosas, etc).
Width of slide block: 150' at road surface
Landcover: Mimosa trees, thick trumpet vines, Willows.
Desiccation crack: None noticeable
Rainfall before the trip date: 1.35", Mesonet Location = Eufala, May 1-24, 2012.
Type of slip surface: Circular

Visual Classification of Soil: reddish brown fat clay, with silt; Hit refusal at 3.5' Took water contents every foot until refusal.

Table_APX_B 10: Route 2, 4 miles south of Route 31 jct

Depth (ft)	% water content	Visual Classification
1	15.18	Light brown/tan mottled silty clay
2	16.01	
3	20.51	
3.5		Auger refusal

Slide notes: This slide area had large (3'+) rocks dumped at the toe of the slide for about 150' to attempt to stop the slide plus the road was slightly realigned. There is also about 2 feet thick of asphalt at the top just outside the guardrails. The edge of the old pavement is about 11 feet from the existing guardrail. The maintenance engineer cannot remember the last time this site was repaired, which means that the slide is moving pretty slowly.

Figure_APX_B 31. Route 2, 4 miles south of junction with Route 31, pavement overlay depth in active slide.

Figure_APX_B 32. Route 2, 4 miles south of junction with Route 31, headscarp in active slide.

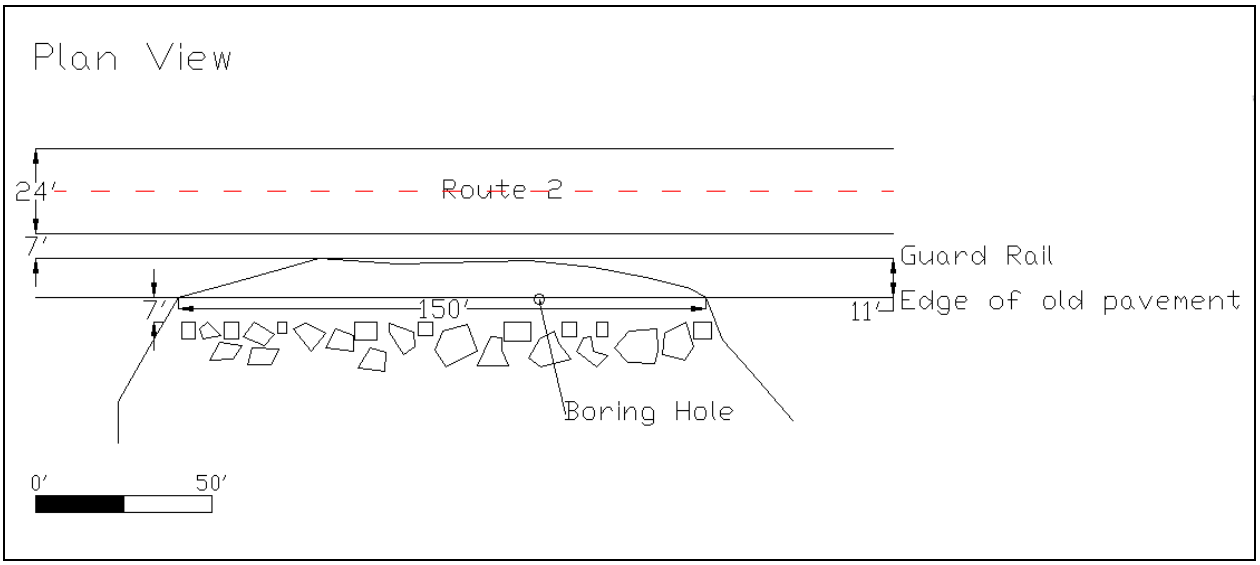

Figure_APX_B 33. Route 2 Landslide

Stop 3: West side of Route 10, about 5 miles south of the intersection with Route 62 (south of Fort Gibson). Reflective guardrails denote sliding area.

Lat: 35°47’21”N
Long: 95°14’3”W

Height of Slope: very steep and covered in dense vegetation
Width of slide block: Difficult to see outline of slide since roadway was realigned.
Landcover: Large diameter deciduous trees (oaks);
Desiccation crack: None noticeable
Rainfall before the trip date: 0.94”, Mesonet Location = Porter, May 1-24, 2012.

Type of slip surface: Most likely circular

Visual Classification of Soil: Slope was too steep to hand auger.

Slide notes: According to the Division 1 maintenance engineer, this is an active slide, where the remediation was large rip rap (3’+) rocks placed at the toe of the slide area, and asphalt overlays to bring the road to the correct elevation. This is still a problem area at the south end of repair. Note cracks appearing in southbound and crossing over into the northbound lane. There are also a concrete ditch and reflective barrier as the guardrail denoting the slide area.

Figure_APX_B 34. West side of Route 10, looking south, realignment is evident. Outline of slide is difficult to see.

Figure_APX_B 35. West side of Route 10, standing on south side of slide area looking north, new overlay is evident.

Figure_APX_B 36. West side of Route 10, south side of reflective guardrail, circular cracking is evident. No riprap at toe in this location.

Stop 4: Route 80 just south of Fort Gibson Dam, on west side of Route 80N

Lat: 35°54’58”N
Long: 95°16’5”W

Height of Slope: Very steep (get height from topo map of area)
Width of slide block: hard to tell, since the overlay of the road is >300’, but no cracking seen.
Landcover: Large diameter deciduous trees (>3’ oaks)
Desiccation crack: None noticeable
Rainfall before the trip date: 0.94”, Mesonet Location = Porter, May 1-24, 2012.
Type of slip surface: May be shallow slide over rocks, since rock outcropping is prevalent.

Visual Classification of Soil: NA

Slide notes: This is a very steep area, with large rock outcroppings on east side of road. Division engineer noted that the road was moved into the mountain (east) in 1988, and rip rap was placed at toe to attempt to stop the sliding. There was approximately 3’ of visible asphalt overlays throughout the slide area. The division engineer said the repairs happened years ago (1988), including drainage, beaver slides, and nothing has been done in recent history. This slide seems to be continuing at a very small rate per year.

Figure_APX_B 37. Looking toward Fort Gibson Dam, slide is on left (west).

Figure_APX_B 38. Route 80 just south of Fort Gibson Dam, 3’ of overlay in middle of slide area.

Figure_APX_B 39. Looking south on Route 80 N (away from dam), shoulder cracking is seen, as well as overlay

Stop 5: Route 75, 0.6 miles north of Preston Road at the first guard rail on right (east). The slide is not visible from road, but there is cracking in the shoulder.

Lat: 35°43'25"N
Long: 95°59'55"W

Height of Slope: Probably 15 feet
Width of slide block: ~40 feet (but did not measure this)
Landcover: Grasses
Desiccation crack: None noticeable
Rainfall before the trip date: 1.2", Mesonet Location = Okmulgee, May 1-24, 2012.
Type of slip surface: Classic Circular. Look at the headscarp.

Visual Classification of Soil: NA

Slide notes: This slide is located on the east side of Route 75 Northbound, 0.6 miles north of the intersection with Preston Road. At the first eastside guardrail north of this intersection, the slide is located at the very north of the guardrail. The project team could not see it from the road, although there was significant cracking in the shoulder inside the guard rail. The landslide is a classic circular failure with a head scarp approximately 5 feet from the edge of the shoulder. The slide seems to be retrogressing toward the road. This slide is directly beneath the power lines. This area may be a problem in the future if the erosion from the headscarp/additional sliding is not taken care of.

Figure_APX_B 40. Route 75, 0.6 miles north of Preston Road, slide area is well defined, toward north end of guardrail, where the natural tree toe support ends.

Figure_APX_B 41. Route 75, 0.6 miles north of Preston Road, looking southbound, shoulder cracking is evident.

Figure_APX_B 42. Route 75, 0.6 miles north of Preston Road, proximity of headscarp to guardrail. Note end of trees/toe support is where slide occurred.

Figure_APX_B 43. Route 75, 0.6 miles north of Preston Road, 2012 Google Earth Satellite Photo of Slide Area.